Quantum chaos

between order and disorder

A selection of papers compiled and introduced by

GIULIO CASATI
Dipartimento di Fisica, Università di Milano

BORIS CHIRIKOV
Budker Institute of Nuclear Physics, Novosibirsk, Russia

CAMBRIDGE
UNIVERSITY PRESS

Published by the Press Syndicate of the University of Cambridge
The Pitt Building, Trumpington Street, Cambridge CB2 1RP
40 West 20th Street, New York, NY 10011-4211, USA
10 Stamford Road, Oakleigh, Melbourne 3166, Australia

First published 1995

Printed in Great Britain at the University Press, Cambridge

A catalogue record of this book is available from the British Library

Library of Congress cataloguing in publication data

Quantum chaos : between order and disorder : a paper selection
compiled and introduced by Giulio Casati, Boris Chirikov.
p. cm.
ISBN 0-521-43291-X
1. Quantum chaos. I. Casati, Giulio, 1942– , II. Chirikov, B.
V. (Boris Valerianovich)
QC174.17.C45Q36 1995
530.1′2–dc20 93-37135 CIP

ISBN 0 521 43291 X hardback

TAG

Contents

Preface

This volume presents a collection of basic papers, some already published others specially written for this volume, devoted to the study of a new phenomenon, the so-called quantum chaos. This problem arose from the by now, well known, classical dynamical chaos. However, unlike the latter, the study of quantum chaos is still in its early stages, attracting the ever growing interest of many physicists (but, unfortunately, of many fewer, as yet, mathematicians).

The original intention, of physicists at least, was mainly to understand the very important generic phenomenon of classical chaos from the viewpoint of the more deep and general quantum mechanics. At first sight it might seem that quantum chaos is simply a particular case of the general phenomenon of dynamical chaos in the well developed ergodic theory of dynamical systems; or it might be a trivial implication of the correspondence principle. Yet, Nature has turned out to be much more tricky, and more interesting!

As the present collection of papers clearly shows, there is no classical-like chaos at all in quantum mechanics. On the other hand since Nature, as is commonly accepted, obeys quantum mechanics, what is then the physical meaning of dynamical chaos? As a result of this surprising obstacle, the general situation in the study of quantum chaos, in the present state of research, might be characterized as some confusion and disorganization which is of course a typical situation in the early stages of a new field of scientific research. It greatly stimulates and encourages the active search for new approaches to the problem, quite often without any attempts to reconcile the different conceptions. The primary goal of this collection is just to help in the cure of such a disease of growth.

For the reader's convenience we have grouped the papers into four different main topics: a) "Classical chaos and quantum localization" which is the most extensively investigated subject; b) "Atoms in magnetic and microwave fields" which refers also to the laboratory experiments in quantum chaos; c) "Semi-classical approximations" which examines the transition between classical and quantum chaos; and d) "Level statistics and random matrix theory" which describes the relation with the well developed statistical theory of complex quantum systems.

The collection of papers is preceded by an introductory chapter in which we

try to link different approaches to the problem of quantum chaos guided by our current personal understanding of this new field.

We thank Anna Auguadro for her valuable assistance in the preparation of this volume.

Novosibirsk – Como

GIULIO CASATI
BORIS CHIRIKOV

Acknowledgments

The following articles in this collection have already been published in the sources shown:

G. CASATI, B. V. CHIRIKOV, F. M. IZRAILEV and J. FORD
Stochastic behaviour of a quantum pendulum under a periodic perturbation
in Lecture Notes in Physics, **93**, *p 334–52 (1979), reproduced by permission Springer-Verlag, Heidelberg*

D. R. GREMPEL, R. E. PRANGE and S. E. FISHMAN
Quantum dynamics of a nonintegrable system
in Physical Review, A**29**, *1639–47 (1984), reproduced by permission of The American Physical Society, New York*

R. BLÜMEL, S. FISHMAN and U. SMILANSKY
Excitation of molecular rotation by periodic microwave pulses. A testing ground for Anderson localization
in the Journal of Chemical Physics, **84**, *2604–14 (1986), reproduced by permission of The American Institute of Physics, New York*

D. L. SHEPELYANSKY
Localization of diffusive excitation in multi-level systems
in Physica, **28**D, *103–14 (1987), reproduced by permission of North-Holland Physics Publishing, Amsterdam*

F. HAAKE, M. KUS and R. SCHARF
Classical and quantum chaos for a kicked top
in Zeitschrift für Physik, B**65**, *381–95 (1987), reproduced by permission of Springer-Verlag, Heidelberg*

L. E. REICHL and L. HAOMING
Self-similarity in quantum dynamics
in Physical Review, A**42**, *4543–61, (1990), reproduced by permission of The American Physical Society, New York*

E. OTT, T. M. ANTONSEN JR and J. HANSON
Effect of noise on time-dependent quantum chaos
in Physical Review Letters, **53**, *2187–90, (1984), reproduced by permission of The American Physical Society, New York*

R. F. GRAHAM
Dynamical localization, dissipation and noise
in the Proceedings of the Varenna Summer School on Quantum Chaos, 1991, *reproduced by permission of the Italian Physical Society*

J. E. BAYFIELD, G. CASATI, I. GUARNERI and D. W. SOKOL
Localization of classically chaotic diffusion for hydrogen atoms in microwave fields
in Physical Review Letters, **63**, *364–7, (1989), reproduced by permission of The American Physical Society, New York*

R. V. JENSEN, M. M. SANDERS, M. SARACENO and B. SUNDARAM
Inhibition of quantum transport due to 'scars' of unstable periodic orbits
in Physical Review Letters, **63**, *2771–5 (1989), reproduced by permssion of The American Physical Society, New York*

C.-H. IU, G. R. WELCH, M. M. KASH, D. KLEPPNER, D. DELANDE and J. C. GAY
Diamagnetic Rydberg atom: confrontation of calculated and observed spectra
in Physical Review Letters, **66**, *145–8, (1991), reproduced by permission of The American Physical Society, New York*

D. WINTGEN, K. RICHTER and G. TANNER
The semiclassical helium atom
in Chaos, **2**, *19–32, (1992), reproduced by permission of The American Institue of Physics, New York*

M. V. BERRY
Semiclassical theory of spectral rigidity
in the Proceedings of the Royal Society, A**400**, *229–51 (1985), reproduced by permission of The Royal Society, London*

M. A. SEPULVEDA, S. TOMSOVIC and E. J. HELLER
Semiclassical propagation: how long can it last?
in Physical Review Letters, **69**, *402–5 (1992), reproduced by permission of The American Physical Society, New York*

N. L. BALAZS and A. VOROS
The quantized baker's transformation
in Annals of Physics, **190**, *1–31 (1989), reproduced by permission of Academic Press, New York*

M. SARACENO
Classical structures in the quantized baker transformation
in Annals of Physics, **199**, *37–60, (1989), reproduced by permission of Academic Press, New York*

O. BOHIGAS, M. J. GIANNONI and C. SCHMIT
Characterization of chaotic quantum spectra and universality of level fluctuation laws
in Physical Review Letters, **52**, *1–4 (1983), reproduced by permission of The American Physical Society, New York*

Introduction

The legacy of chaos in quantum mechanics

G. CASATI
Dipartimento di Fisica, Università di Milano
Via Castelnuovo – 22100 Como, Italy

B. CHIRIKOV
Budker Institute of Nuclear Physics
630090 Novosibisrk 90, Russia

The present collection of papers is devoted to a rather new and very controversial topic, the so-called "quantum chaos". Some researchers see nothing essentially new at all in this phenomenon (apart from a number of various examples and models), and they have good reason to believe so. Indeed, the problems in this field all belong to the traditional, "old-fashion", and rather "simple" quantum mechanics of finite-dimensional systems with a given interaction and no quantized fields.

Nevertheless, many, including ourselves, consider quantum chaos to be a new discovery, though in an old field, of a great importance for fundamental physics. To understand this, the phenomenon of quantum chaos should be put into its proper perspective in recent developments in physics. The central point of this perspective is the conception of dynamical chaos (also a rather new topic) in classical mechanics (for a good review see, e.g., Refs.[1-3]). Thus before discussing the current understanding of quantum chaos we need briefly to describe classical dynamical chaos.

1 Dynamical chaos in classical mechanics

The conception of dynamical chaos destroys the deterministic image of the classical physics and shows that typically the trajectories of the deterministic equations of motion are in some sense random and unpredictable. The mechanism for such a surprising property of classical mechanics is related to the most strong (exponential) local instability of motion. In what follows we restrict ourselves to Hamiltonian (non-dissipative) systems as more fundamental. The local instability is described by the linearized equations of motion:

$$\left.\begin{aligned} \dot{\xi} &= \left(\frac{\partial^2 H}{\partial p \partial q}\right)_r \xi \quad + \left(\frac{\partial^2 H}{\partial p^2}\right)_r \eta \\ \dot{\eta} &= -\left(\frac{\partial^2 H}{\partial q^2}\right)_r \xi \quad - \left(\frac{\partial^2 H}{\partial q \partial p}\right)_r \eta \end{aligned}\right\} \tag{1}$$

where $H = H(q, p, t)$ is the Hamiltonian; q, p are N-dimensional vectors in the phase space and $\xi = dq$, $\eta = dp$ are N-dimensional vectors in the tangent space.

The coefficients of the linear equations (1) are taken on the reference trajectory and hence explicitly depend on time. This dependence is generally very complicated if, for example, the reference trajectory is chaotic.

The stability of the motion on the reference trajectory is characterized by the maximal Lyapunov exponent defined as the limit

$$\Lambda = \lim_{|t|\to\infty} \frac{1}{|t|} \ln d(t) \tag{2}$$

where $d^2 = \xi^2 + \eta^2$ is the length of the tangent vector and where $d(0) = 1$ is assumed.

The exponential instability of motion means positive maximal Lyapunov exponent $\Lambda > 0$. Notice that in Hamiltonian systems the instability does not depend on the direction of time and, hence, is reversible as is the chaotic motion.

The reason why the exponentially unstable motion is called chaotic is in that almost all trajectories of such a motion are unpredictable in the following sense: according to the Alekseev–Brudno theorem (see Ref.[4]) in the algorithmic theory of dynamical systems the information $I(t)$ associated with a segment of trajectory of length t is equal asymptotically to

$$\lim_{|t|\to\infty} \frac{I(t)}{|t|} = h = \sum \Lambda_+ \tag{3}$$

where $\sum \Lambda_+$ is the sum of all positive Lyapunov exponents and h is the so-called KS (after Kolmogorov–Sinai) entropy. This important result shows that in order to predict each new segment of a chaotic trajectory one needs an additional information proportional to the length of this segment and independent of the full previous length of trajectory. This means that this information cannot be extracted from observation of the previous motion, even an infinitely long one! If the instability is not exponential but, for example, only a power law, then the required information per unit time is inversely proportional to the full previous length of trajectory and, asymptotically, the prediction becomes possible. Needless to say, for a sufficiently short time interval the prediction is of course possible even for a chaotic system and can be characterized by the randomness parameter [5]

$$r = \frac{h|t|}{|\ln \mu|} \tag{4}$$

where μ is the accuracy of trajectory recording. The prediction is possible in the *finite* interval of "temporary determinism" ($r \lesssim 1$) while $r \gg 1$ corresponds to the *infinite* region of asymptotic randomness.

Notice that the information per unit time (3) does not depend on the accuracy of recording μ which determines the prediction time scale only. Recently a powerful technique has been developed which actually predicts a chaotic trajectory within this limit [6].

The important condition $h > 0$, which characterizes chaotic motion, is not

invariant with respect to the change of time variable. (According to Ref.[3] the only invariant statistical property under change of time variable is ergodicity.) In our opinion the resolution of this difficulty is in that the proper characteristic of motion instability, important for dynamical chaos, should be taken with respect to the oscillation phases whose dynamics determines the nature of the motion. This implies that the proper time variable must vary proportionally with the phases.

The exponential instability implies a continuous spectrum of motion. (In a discrete spectrum the instability can be at most linear in time [57].) The continuous spectrum, in turn, implies correlation decay; this property, which is called mixing in ergodic theory, is the most important property of dynamical motion for the validity of the statistical description. The point is that mixing provides the statistical independence of different parts (sufficiently separated in time) of a dynamical trajectory. This is the main condition for the application of probability theory which allows the calculation of the statistical characteristics such as diffusion, relaxation, distribution functions etc. However, it is not clear as yet whether or not the strongest property of exponential instability is really required for a meaningful statistical description of dynamical motion.

In the modern theory of dynamical systems the latter property corresponds to one limiting case of dynamical motion which is called dynamical chaos (Fig. 1). The opposite limiting case is the so-called completely integrable motion which possesses the full set of N motion integrals (where N is the number of freedoms) in involution and in which, moreover, the action-angle variables can be introduced. The property of complete integrability is very delicate and non-typical as it is destroyed by an arbitrarily weak perturbation which converts a completely integrable system into a KAM-integrable system [7]. (Unlike integrable motion, chaotic motion is very robust: it is structurally stable and is not affected by weak perturbations [58].) The structure of the KAM motion is very intricate; the motion remains completely integrable for most initial conditions yet a single, connected, chaotic motion component (for $N > 2$) arises of exponentially small (with respect to perturbation) measure which is nevertheless everywhere dense. Interesting enough, the chaotic trajectories in this component approach arbitrarily close to any point on the energy surface, yet the motion is non ergodic due to the positive measure of the stable component. Ergodicity means that almost all trajectories not only approach every point on the energy surface, but cover it homogeneously that is the sojourn time of a trajectory in any region of phase space is proportional to its invariant measure. The property of ergodicity which has given the name to the whole ergodic theory turned out to be neither necessary nor sufficient for the statistical description. Indeed chaotic components of the motion may cover only a part of the energy surface (which is rather a typical case in dynamical systems); on the other hand for a meaningful statistical description a mixing property is needed which provides the relaxation to some statistical steady state.

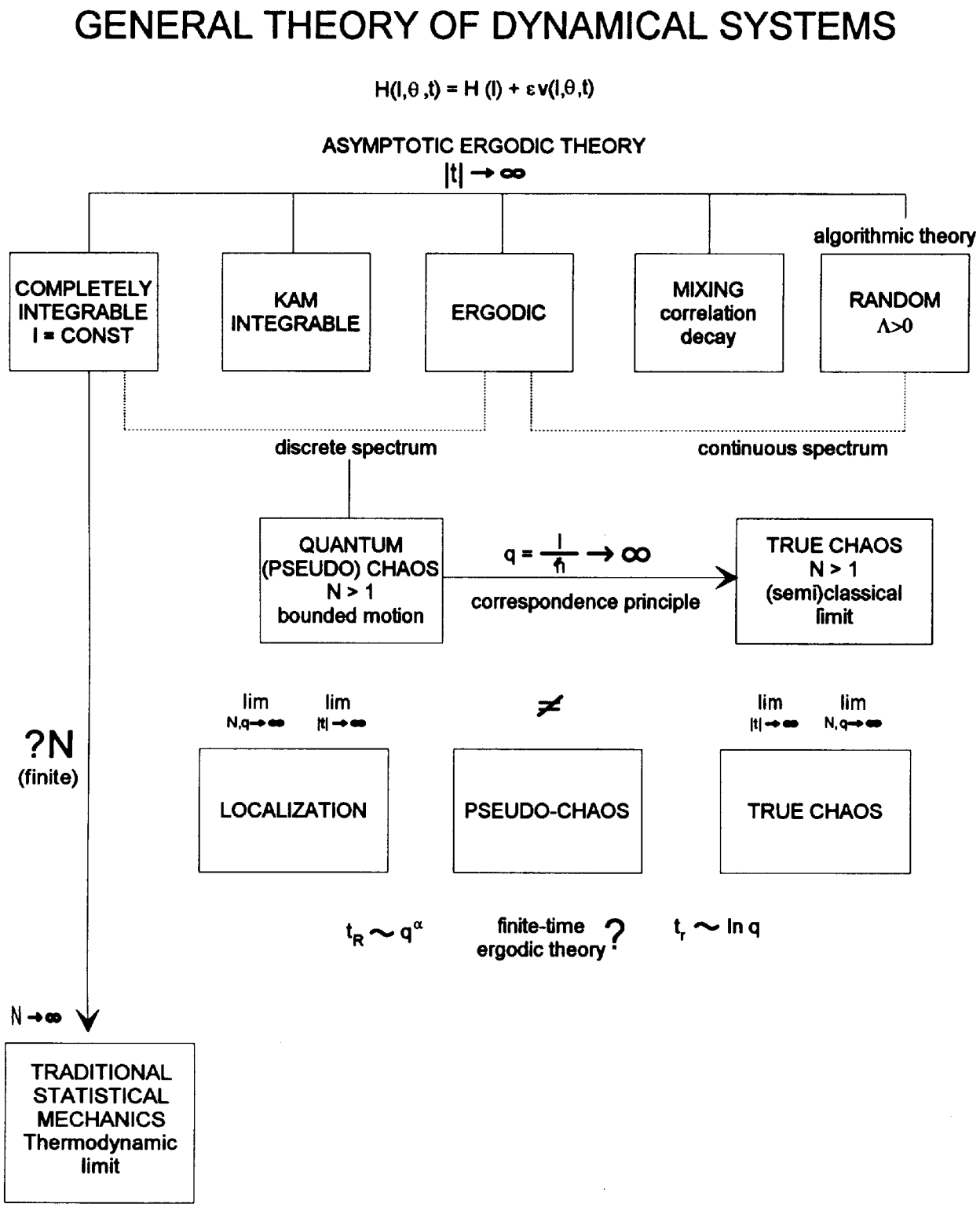

Fig. 1. The place of quantum chaos in modern theories: action-angle variables I, θ; number of freedoms N; Lyapunov exponent Λ; quasiclassical parameter q; time scales t_R and t_r; Planck's constant $\hbar$. Two question marks indicate the problems in a new ergodic theory non-asymptotic in N and $|\ t\ |$ (see also section 10).

Instead in terms of trajectories an equivalent description of classical dynamics can be given by means of distribution functions which, if non-singular, represent not a single trajectory but a continuum of them. As is well known the distribution function obeys a linear Liouville equation. Thus the condition of non-linearity for dynamical chaos to occur is restricted to the description in terms of trajectories where the rôle of non-linearity is to bound the linearly unstable motion. In terms of distribution functions ergodicity means that the time-averaged distribution function is constant with respect to the invariant measure. Instead, the stronger property of mixing implies the approach, on average, of any initially smooth distribution to a steady-state. This process is called *statistical relaxation.* The relaxation is of course time-reversible as is the motion along a particular trajectory. However, unlike the latter, the evolution of the distribution function is non recurrent. Notice that according to the Poincaré theorem the trajectory recurs infinitely many times independent of the type of motion (regular or chaotic); the difference is that for regular motion the recurrence time is strictly bounded from above whereas in the latter case arbitrarily large recurrence times are possible. The time-reversibility of the distribution function is related to its very complicated structure which becomes more and more "scarred" as the relaxation proceeds. In the case of exponential instability of motion the spatial scale of the oscillations also decreases exponentially with time. It is in these fine spatial oscillations that the memory of the initial state is retained forever, which is only possible in a continuous phase space.

To get rid of this complicated structure, the distribution function must be "coarse-grained", that is, averaged on some domain. The evolution of the coarse-grained function is described by a kinetic equation, e.g., a diffusion equation. The coarse-grained function converges to a smooth steady state which is a constant with respect to the invariant measure.

In closing this section we would like to stress again the two crucial properties of classical mechanics necessary for dynamical chaos to occur: (i) a continuous spectrum of the motion, and (ii) a continuous phase space.

2 Quantum chaos vs the correspondence principle

The problem of quantum chaos arose from the attempts to understand the very peculiar phenomenon of classical dynamical chaos in terms of quantum mechanics. Preliminary investigations immediately unveiled a very deep difficulty related to the fact that the above mentioned conditions for classical chaos are violated in quantum mechanics. Indeed the energy and the frequency spectrum of any quantum motion, bounded in phase space, are always discrete. According to the existing theory of dynamical systems such motion corresponds to the limiting case of regular motion. The ultimate origin of this fundamental quantum property is discreteness of the phase space itself or, in modern mathematical language, a non-commutative geometry of the latter. This is the very basis of all quantum

physics directly related to the fundamental uncertainty principle which implies a finite size of an elementary phase-space cell: $\Delta x \cdot \Delta p \gtrsim \hbar$ (per freedom).

The naive resolution of this difficulty would be the absence of any quantum chaos. For this reason it was even proposed to use the term "quantum chaology" [8] which essentially means the study of the absence of chaos in quantum mechanics. If the above conclusion were true, a sharp contradiction would arise with the correspondence principle which requires the transition from quantum to classical mechanics for all phenomena including the new one: dynamical chaos. Does this really mean a failure of the correspondence principle as some authors insist (see, e.g., Ref.[9]) ? If it were so quantum chaos would, indeed, be a great discovery since it would mean that classical mechanics is not the limiting case of quantum mechanics but a different separate theory. "Unfortunately", there exists a less radical (but also interesting and important) resolution of this difficulty which is discussed below.

A recent breakthrough in the understanding of quantum chaos has been achieved, particularly, due to a new philosophy which, either explicitly or implicitly, is generally accepted; namely the whole physical problem of quantum dynamics is considered as divided into two qualitatively different parts:

(i) proper quantum dynamics as described by a specific dynamical variable, the wavefunction $\psi(t)$; and

(ii) quantum measurement including the recording of the result and hence the collapse of the ψ function.

The first part is described by some deterministic equation, for example, the Schrödinger equation and naturally belongs to the general theory of dynamical systems. The problem is well posed and this allows for extensive studies. In the following, as well as in all papers of the present collection only the first part is discussed.

The second part still remains very vague to the extent that there is no common agreement even on the question whether this is a real physical problem or an ill-posed one so that the Copenhagen interpretation of (or convention in) quantum mechanics gives satisfactory answers to all the admissible questions. In any event there exists as yet no dynamical description of quantum measurement including the ψ-collapse.

The absence of classical-like chaos is true for the above mentioned first part of quantum dynamics only. Quantum measurement as far as the result is concerned, is fundamentally a random process. However, there are good reasons to believe that this randomness can be interpreted as a particular manifestation of dynamical chaos [10].

The separation of the first part of quantum dynamics, which is very natural from a mathematical viewpoint, was introduced and emphasized by Schrödinger who, however, certainly underestimated the importance of the second part in physics.

3 Characteristic time scales of quantum chaos

3.1 The models

One way to reconcile the discrete spectrum with the correspondence principle is to introduce some characteristic time scales of quantum motion. The main idea is that the distinction between discrete and continuous spectra is non ambiguous in the limit $t \to \infty$ only. This idea was suggested by our first numerical experiments in quantum chaos in which a very simple model was used (the so-called "kicked rotator")[11]. In the classical limit this model is described by the Hamiltonian

$$H = \frac{n^2}{2} + k \cdot \cos \vartheta \cdot \delta_T(t) \tag{5}$$

where (n, ϑ) are action-angle variables, k and T are the strength and period of the perturbation, and $\delta_T(t)$ is the δ-function of period T. The corresponding equations of motions are given by the so-called standard map (SM)

$$\left.\begin{aligned} \bar{n} &= n + k \sin \vartheta \\ \bar{\vartheta} &= \vartheta + \bar{n}\, T \end{aligned}\right\} \tag{6}$$

The only parameter of this map is $K = kT$.

For $K < 1$ the motion is strictly bounded while for $K \gg 1$ it is ergodic, mixing and exponentially unstable with a Lyapunov exponent per step:

$$\Lambda \approx \ln \frac{K}{2} \tag{7}$$

This model can be considered either on the infinite cylinder (unbounded motion) or on a finite torus (bounded motion) of circumference

$$L = \frac{2\pi m}{T} \tag{8}$$

where m is an integer to avoid discontinuities.

The SM is very popular in studies of dynamical chaos both classical and quantal because of its apparent simplicity and intrinsic richness. (The nickname "kicked rotator" is related to a particular physical interpretation of this model as a rotator with angular momentum n driven by a series of periodic pulses, or "kicks".) Yet, it can also be considered also as the Poincare surface-of-section map for a conservative system of two freedoms. Particularly, the map on a torus (8) models the energy shell of a conservative system which is the quantum counterpart of the classical energy surface. What makes the SM almost universal is the local (in momentum) approximation it provides for a broad class of more complicated physical models.

One well studied example of such models is the photoeffect in Rydberg atoms.

The main features of this problem are described by the one-dimensional Hamiltonian [12] (see also Section.7)

$$H = -\frac{1}{2n^2} + \epsilon z\,(n, \vartheta)\cos\omega t \tag{9}$$

where ϵ and ω are the strength and the frequency of the linearly polarized electric field, n, ϑ are the action-angle variables and z the coordinate along the field direction.

If the field frequency exceeds the electron frequency the motion of system (9) is approximately described by a map over one Kepler period of the electron, the so-called Kepler map:

$$\bar{v} = v + k\cdot\sin\phi\,; \qquad \bar{\phi} = \phi + \frac{\pi}{\sqrt{2\omega}}(-\bar{v})^{-3/2} \tag{10}$$

where $v = E/\omega = -(2\omega n^2)^{-1}$, ϕ is the field phase at perihelion and k is perturbation parameter (in atomic units)

$$k \approx 2.58\,\frac{\varepsilon}{\omega^{5/3}} \tag{11}$$

Linearizing the second Eq.(10) in v reduces the Kepler map to the SM (6) with the same k, and parameter

$$T = 6\pi\omega^2 n^5 \tag{12}$$

provided $k \ll v$. Thus, the SM describes the dynamics locally in momentum. In this particular model the momentum v is proportional to the energy E as the conjugate phase ϕ is proportional to time.

Interestingly, the Kepler map can be derived from a simple expression for the electron free fall on the Coulomb center which, in reversed time, reads:

$$z = \left(\frac{3}{\sqrt{2}}\right)^{2/3} t^{2/3}$$

Then, the perturbation parameter is given by the integral

$$k = -2\varepsilon\int_0^\infty z(t)\cdot\cos\omega t\,dt = (48)^{1/6}\,\Gamma(2/3)\cdot\frac{\varepsilon}{\omega^{5/3}} \approx 2.58\frac{\varepsilon}{\omega^{5/3}} \tag{13}$$

Another, less known, example is the "kicked top", or the spin dynamics on a sphere [13] which is described by the Hamiltonian (cf. Eq.(5)):

$$H = \frac{s_z^2}{2} + \frac{k_0}{s}\cdot s_x\cdot\delta_T(t) = \frac{s_z^2}{2} + k_0\sqrt{1-\frac{s_z^2}{s^2}}\cos\varphi\cdot\delta_T(t) \tag{14}$$

where s_z, s_x are the components of spin whose modulus squared $s^2 = s_z^2 + s_x^2 + s_y^2 = const$ is the motion integral, and φ is the azimuthal angle canonically conjugated to the momentum $s_z = s\cdot\cos\theta$ where θ is the polar angle. As is easily verified, the invariant measure $ds_x\cdot ds_y\cdot ds_z = s\,ds\cdot ds_z\cdot d\varphi$ is proportional to the area on the sphere.

If $k_0 \ll s$ the spin dynamics can be approximately described by the SM with the perturbation parameter

$$k(s_z) = k_0 \sqrt{1 - \frac{s_z^2}{s^2}} \tag{15}$$

depending on action s_z. This approximation is valid if the change Δk of k in one kick is less than k. This is true on the whole sphere except a narrow 'polar' region

$$\frac{s - s_z}{s} \lesssim \left(\frac{k_0}{s}\right)^2 << 1 \tag{16}$$

The restriction $s_z \ll s$ [14] is therefore not necessary.

An interesting version of this model [15] is the motion on a hyperboloid

$$s_x^2 + s_y^2 - s_z^2 = \pm s^2 \tag{17}$$

In this case the SM perturbation parameter becomes

$$k(s_z) = k_0 \sqrt{\frac{s_z^2}{s^2} \pm 1} \tag{18}$$

where the sign coincides with that of motion integral (17).

The local description via the SM allows the determination of the chaos border in all these models from the condition

$$K = T\,k(s_z) \approx 1 \tag{19}$$

The statistical properties of the SM are described by a diffusion in action n with the rate

$$D_0 = \frac{<(\Delta n)^2>}{\tau} = \frac{k^2}{2} C(K) \tag{20}$$

where the integer time $\tau = t/T$ is the number of map iterations, and the function $C(K)$ accounts for dynamical correlations. Particularly, $C(K) \to 1$ for $K \gg 1$, and $C(K) \to 0$ at the chaos border (19). The diffusion Green function is Gaussian

$$g(n, \tau) = \frac{\exp\left(-\dfrac{(n - n_0)^2}{2D_0\tau}\right)}{\sqrt{2\pi D_0 \tau}} \tag{21}$$

For the bounded SM (on a torus) the diffusion leads to the statistical relaxation of any non-singular distribution function to the ergodic state:

$$f(n) \to \frac{1}{L} \tag{22}$$

with a characteristic time $\tau_{cl} \sim L^2/D_0$.

The quantized standard map (QSM) on a cylinder, first introduced in Ref.[11], is described by the relation:

$$\overline{\psi} = \hat{U}\,\psi = \exp(-ik\,\cos\,\hat{\vartheta}) \cdot \exp(-i\,\frac{T}{2}\,\hat{n}^2)\,\psi \tag{23}$$

where $\hat{U}$ is a unitary operator, $\hat{n} = -i\partial/\partial\vartheta$, and $\hbar = 1$. Notice that, while for the bounded classical SM on a torus (8) the only change is to take n *mod* L, for the QSM expression (23) becomes more complicated [16].

If $k \gg 1$ the perturbation couples approximately $2k$ unperturbed states per iteration of map (23). For $k \ll 1$ all the transitions are suppressed. Thus, $k \sim 1$ is a specific border of quantum stability due to the discrete spectrum and is independent of the behaviour in the classical limit [61,11]. This is also called the *perturbative localization border.*

For the spin model the unitary operator is obtained from the first expression of Hamiltonian (14):

$$\overline{\psi} = \exp(-i\frac{k_0}{s}\hat{s}_x) \cdot \exp(-i\frac{T}{2}\hat{s}_z^2)\psi \tag{24}$$

(The second expression in Eq.(14) is only a quasiclassical approximation for $s \gg 1$. The same is also true for model (17).) The transition to the classical limit corresponds to $k \to \infty$, $T \to 0$, while $K = kT = const$, $LT = const$ (for model (5)) and $k/s = const$, $s_z/s = const$ (for models (14) and (17)).

3.2 *The relaxation time scale*

In Fig. 2(*a*) we show an example of quantum 'diffusion' in the SM ($< n^2 > \sim \tau$). It is seen that during a finite time interval ($\tau \approx 200$) quantum diffusion is close to the classical diffusion (the straight line) in accordance with the correspondence principle. Moreover, during this time interval quantum diffusion follows many other details of classical diffusion as shown in Fig. 3. These are very satisfactory results; however, for longer times something breaks down and quantum diffusion, unlike classical diffusion, completely stops [11,17,18] (Fig. 2(*b*)).

The general explanation of this phenomenon is related to the fundamental uncertainty principle [19]. Indeed, the discrete spectrum cannot be resolved if

$$t \lesssim \rho_0 \sim t_R \tag{25}$$

where t_R is called the *relaxation time scale*, and ρ_0 is the energy (or quasienergy) level density for those eigenstates which are actually present in the initial state $\psi(0)$ and, hence, determine the system's dynamics. We call these *operative eigenstates.*

Generally, $\rho_0 \leq \rho$ where ρ is the total level density. The latter may even be infinite, like for the unbounded SM. On the torus the quasienergy density $\rho = L/(2\pi/T) = m$ which is, surprisingly, a classical quantity that does not change in the quasiclassical transition and which determines the upper bound of the relaxation time scale in continuous time t. This is because the physical time for the model under consideration is the number of map iterations $\tau = t/T$ in which the relaxation time scale

$$\tau_R = \frac{t_R}{T} \sim \frac{\rho_0}{T} \leq \frac{m}{T} \tag{26}$$

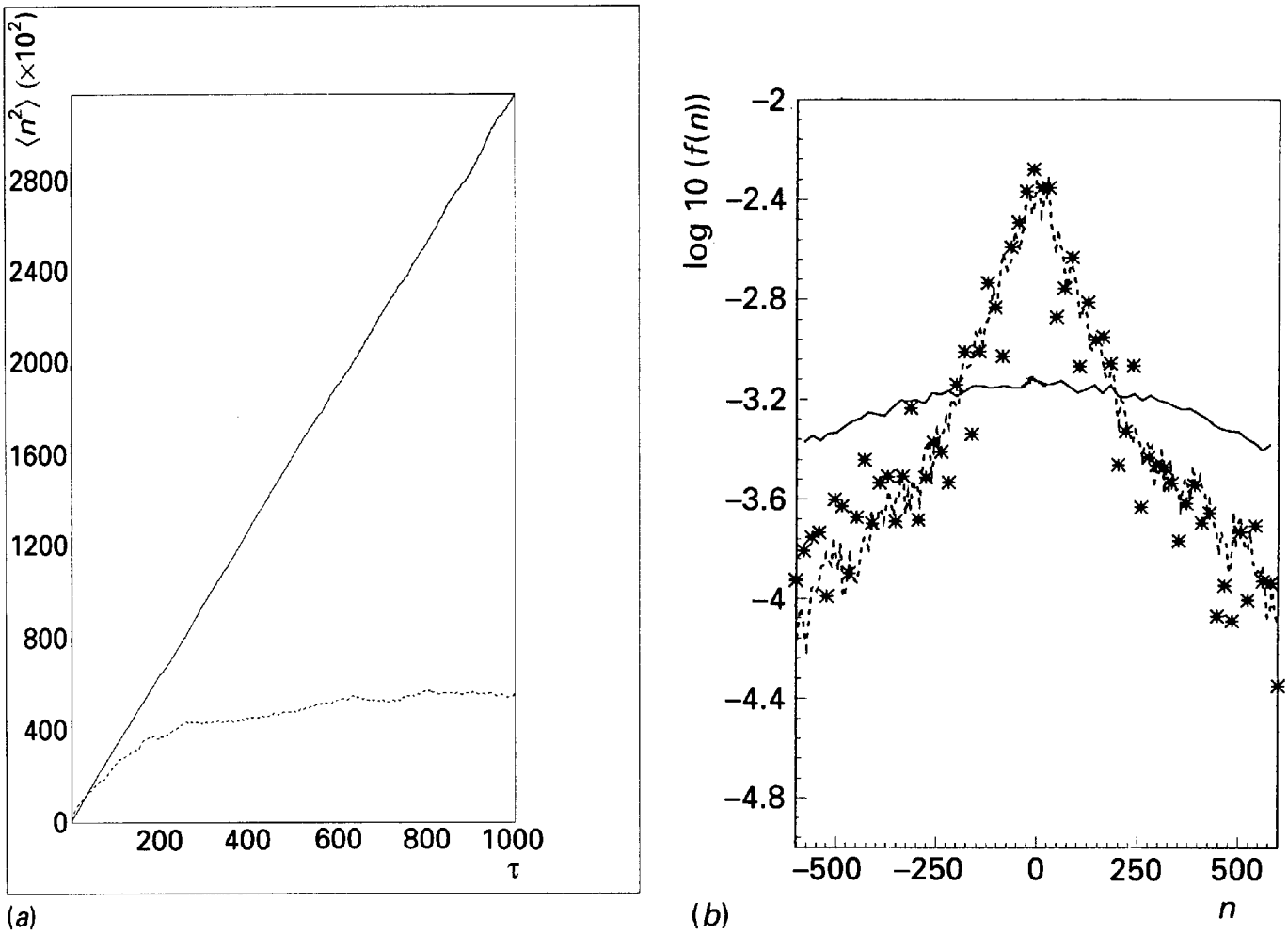

Fig. 2. Classical and quantum diffusion in the SM for $K = 5$, $k = 25$, $T = 0.2$. (*a*) Classical (solid curve) and quantum (dotted curve) unperturbed energy $< n^2(\tau) >= 2E$ as a function of time τ (number of map iterations). (*b*) Classical (solid curve) and quantum (dashed curve) probability distribution after time $\tau = 1000$. The stars give the Husimi distribution integrated over the angle ϑ.

grows indefinitely in the classical limit $T \to 0$, also in accordance with the correspondence principle.

For the kicked rotator the explicit estimate for this time scale has the remarkable form [19]

$$\tau_R \sim D_0 \tag{27}$$

which relates the essentially quantum characteristic τ_R with the classical diffusion rate.

3.3 The random time scale

As discussed above the main peculiarity of quantum chaos is its restriction to a finite time interval: for this reason the term *quantum pseudo-chaos* is sometimes used to distinguish it from the "true" chaos in the classical limit. This is also true for a stronger chaotic property – the exponential instability. Indeed, according to

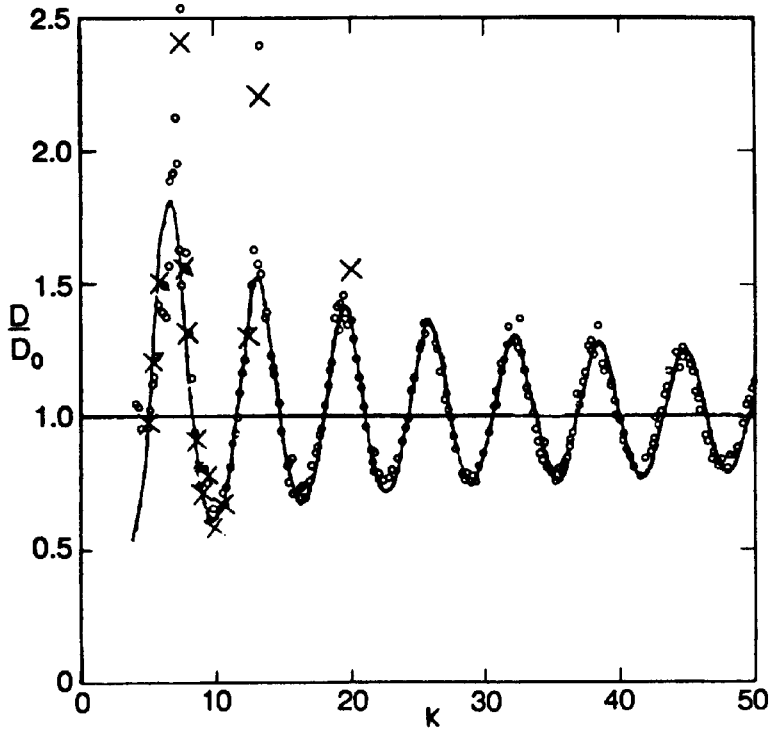

Fig. 3. Classical (circles) and quantum (crosses) diffusion rates in the SM vs the classical parameter K. Here $D_0 = k^2/2$ and the solid curve is the prediction of a simple theory [63]. (From Ref.[43].)

the well-known Ehrenfest theorem, as long as a quantum wave packet remains narrow it follows a beam of classical trajectories. During this time interval the wave-packet motion is as random as the classical trajectory. Particularly the packet is exponentially spreading with the classical rate h. However, the initial size of the quantum packet (unlike in the classical case) is restricted from below by the elementary cell of quantum phase space which is $\sim \hbar$ (equal 1 in our units). The final size for a bounded motion is proportional to some (large) quasiclassical parameter q which is of the order of the characteristic value of the action variable. Therefore, the full time for the exponential spreading of the packet is of the order

$$\tau_r \sim \frac{\ln q}{h} \tag{28}$$

This time scale has been introduced and explained in Ref.[20] (see also Ref.[69]). For the standard map there are two quantum parameters, k and $1/T$. If we consider the optimal, least-spreading, wave packet ($\Delta\vartheta_0 \sim (\Delta n_0)^{-1} \sim \sqrt{T}$) the latter estimate becomes [19]

$$\tau_r \sim \frac{|\ln T|}{\ln \dfrac{K}{2}} \tag{29}$$

This is another time scale, much shorter than τ_R (26), which we call the *random time scale*. It increases indefinitely as $T \to 0$, again in accordance with the correspondence principle.

In Fig. 4 an example of the evolution of an initially narrow wave packet is shown demonstrating both the random ((*a*)–(*c*)) and the relaxation ((*d*)–(*f*)) time scales compared with the classical evolution.

Even though the estimates (28, 29) appear very simple, almost trivial, some questions remain open. One is why only stretching of the packet shows up in Fig.4 without any substantial squeezing (see also Ref.[21]). Apparently, this is related to the particular phase-space density used (the Husimi distribution). Indeed, this density is obtained by the projection of an evolving quantum state on the coherent states whose width is fixed in *both* coordinate and momentum separately whereas the uncertainty principle restricts the product only. The problem is how long this product is going to remain unchanged (particularly minimal) which is the quantum counterpart of the phase-space volume conservation in classical mechanics. To the best of our knowledge, nobody has analysed this as yet. In our understanding, the Wigner function is much more suitable for the study of this problem.

The rate of "inflation" of the phase-space volume occupied by a quantum state can be estimated from the Liouville equation for the Wigner function [22]. In the particular case of the SM it can be written in the quasiclassical region as

$$\frac{dW}{dt} \approx -\frac{1}{24} \cdot \frac{\partial^3 H}{\partial \vartheta^3} \cdot \frac{\partial^3 W}{\partial n^3} \tag{30}$$

To obtain an estimate for the inflation we substitute in the rhs the "unperturbed" classical density $W_0(n, \vartheta, \tau)$ in the form of a Gaussian packet of rms dimensions A and $a \leq A$ with the minimal area $A \cdot a = 1/2$, stretching at angle $T \ll 1$ with the n-axis. Then, $\partial W/\partial n \sim W(T/a)$ while $\partial^3 H/\partial \vartheta^3 \sim k\,\delta_T(t)$, and we obtain from Eq.(30)

$$\frac{d}{d\tau} \ln W \sim k(AT)^3$$

Since $A = A_0 \cdot \exp(\Lambda\tau)$ where $\Lambda = \ln(K/2)$ is the Lyapunov exponent, and $A_0 = \Delta n_0 \sim 1/\sqrt{T}$ for the least spreading packet, we arrive at the estimate

$$\ln \frac{W}{W_0} \sim \frac{k(AT)^3}{\Lambda} \sim 1 \tag{31}$$

which determines the *inflation time scale* τ_{if} and the maximal packet length prior to a substantial inflation $\Delta\vartheta_{if} = (AT)_{if}$:

$$\tau_{if} \sim \frac{|\ln(TK^2/\Lambda^2)|}{6\Lambda}; \qquad \Delta\vartheta_{if} \sim \left(\frac{\Lambda}{k}\right)^{1/3} >> \Delta\vartheta_0 \sim T^{1/2} \tag{32}$$

Another mechanism for the destruction of the unstable quantum packet is related to discrete (integer) values of action n. Apparently, it begins to work for $a \lesssim T$ when the continuous derivative $\dfrac{\partial W}{\partial n}$ breaks down. This determines the *destruction time scale*

$$\tau_d \sim \frac{|\ln T|}{2\Lambda}; \qquad \Delta\vartheta_d \sim 1 \tag{33}$$

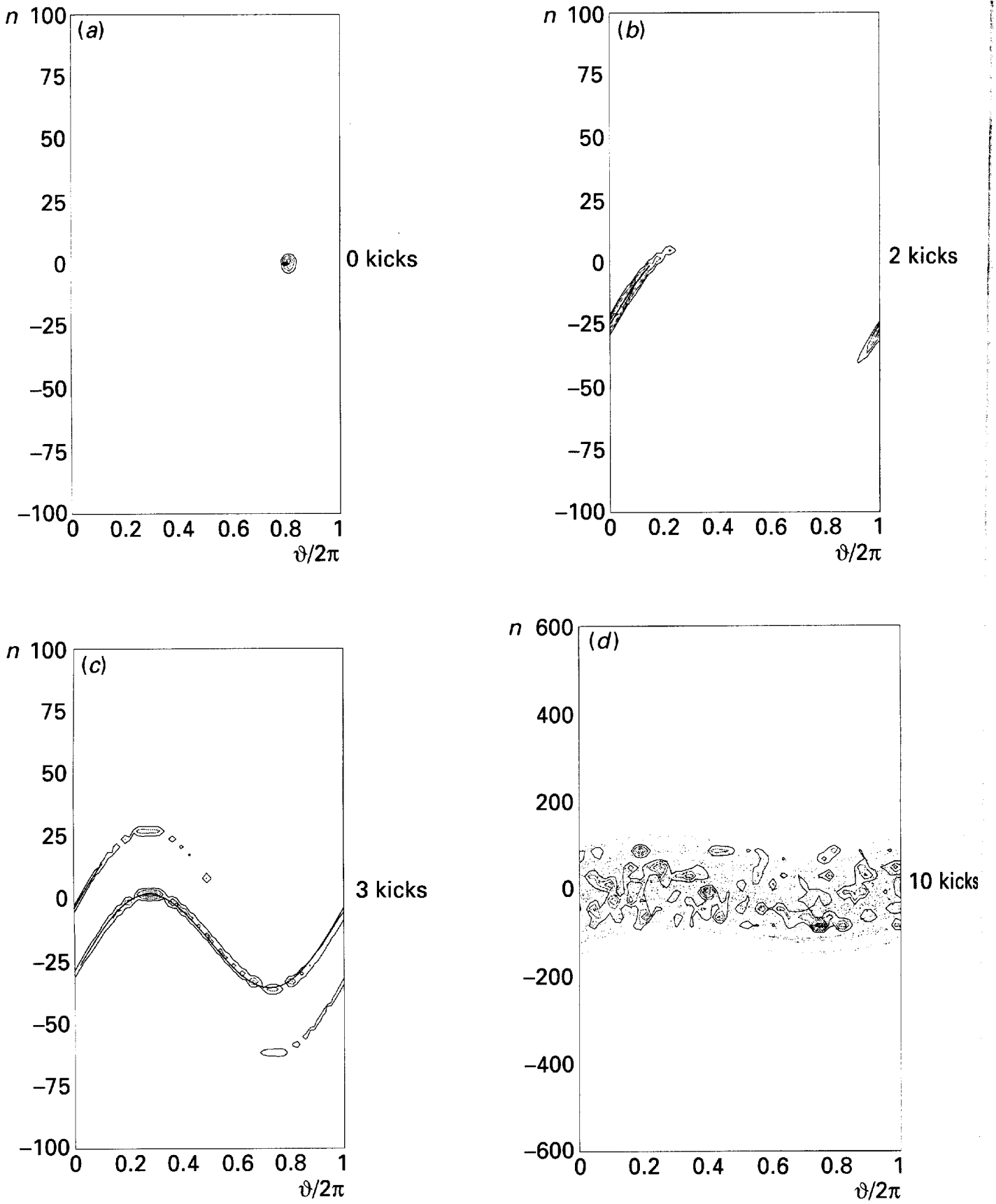

Fig. 4. A comparison between classical and quantum evolution in the kicked rotator for the same parameters as in Fig. 2. The initial quantum state is a coherent packet. As to the classical evolution we considered 2000 trajectories starting in the same area, of size $\hbar(=1)$, occupied by the initial quantum state (Fig. (*a*)). In the following figures ((*b*)–(*f*)), the dots represent the classical trajectories while the curves are level curves of the Husimi distribution. For each figure, taken at different times, we divide by 8 the maximum value of the Husimi distribution by 8 and then plot the seven level curves: (*b*) $\tau = 2$; (*c*) $\tau = 3$; (*d*) $\tau = 10$; (*e*) $\tau = 100$; (*f*) $\tau = 1000$. From this figure, as well as from fig. 2, the quantum localization phenomenon is clearly evident.

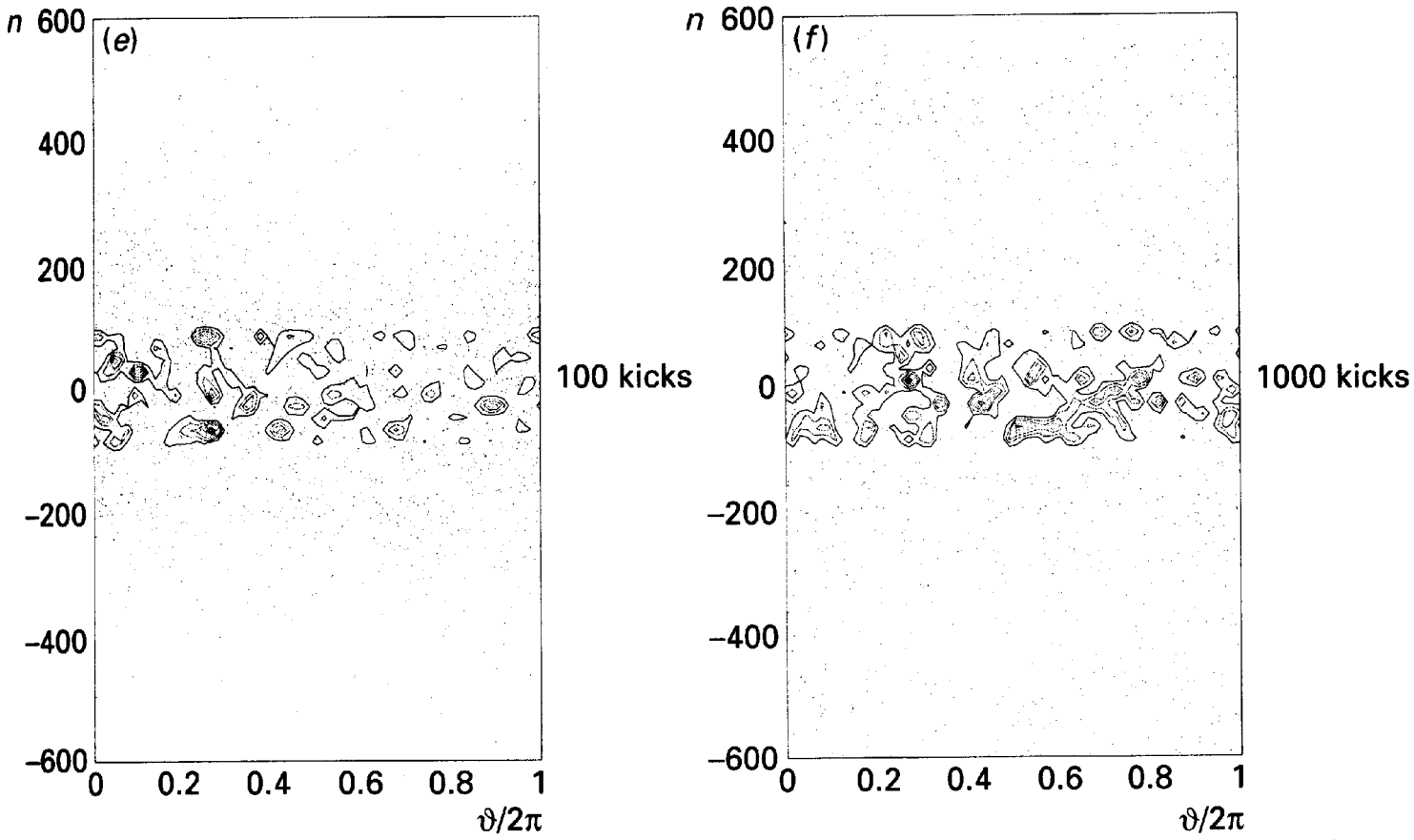

Fig. 4. —*Continued*, for figure caption see previous page

The scales τ_{if} and τ_d are comparable to each other and also to the well-known estimate (29). However, the critical values of the packet length, $\Delta\vartheta_{if}$ and $\Delta\vartheta_d$ are essentially different for $k \to \infty$. The numerical evidence seems to agree better with the destruction, rather than the inflation, mechanism but the latter may be hidden by the Husimi distribution.

We think that the concept of characteristic time scales of quantum dynamics is a satisfactory resolution of the apparent contradiction between the correspondence principle and the quantum transient (finite-time) pseudo-chaos. Some physicists, however, feel that such an explanation is, at least, ambiguous because it includes the two limits which do not commute:

$$\lim_{|t|\to\infty} \lim_{q\to\infty} \neq \lim_{q\to\infty} \lim_{|t|\to\infty}$$

While the first order leads to classical chaos, the second one results in an essentially quantum behaviour with no chaos at all. To resolve these doubts we note that in physics one does not need to take any limit at all, and, in principle, we can describe anything quantum-mechanically. If, nevertheless, we would like to make use of the much simpler classical mechanics (for practical purposes) then only one limit ($q \to \infty$) is quite sufficient as the physical time is certainly finite. Finally, even if it would be helpful for some reason (e.g., for mathematical convenience) formally to take the limit $|t| \to \infty$ this should be *conditional;* namely, one should

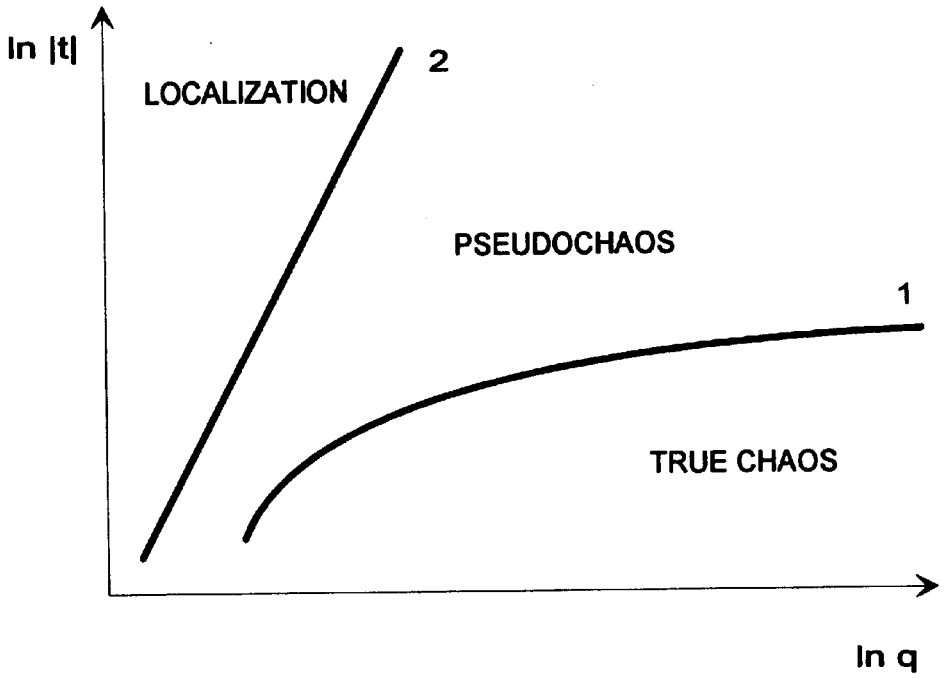

Fig. 5. Time scales of classically chaotic quantum motion: curve 1 - random time scale $t_r \sim \ln q$; curve 2 - relaxation time scale $t_R \sim q^\alpha$; $q \gg 1$ is the quasiclassical parameter.

keep the ratio $|t|/t_R(q)$ or $|t|/t_r(q)$ fixed. In other words the two above limits should be taken simultaneously. The general structure of quantum dynamics on the plane (q, t) is outlined in Fig. 5.

The limit $|t| \to \infty$ is related to the existing ergodic theory which is asymptotic in t. Meanwhile the new phenomenon of quantum chaos requires the modification of the theory to a finite time which is a difficult mathematical problem still to be solved. On the other hand, the practical importance of statistical laws even for a finite time interval is that they provide a relatively simple description of the *essential* behaviour for a very complicated dynamics.

In any event, if quantum mechanics is the universal theory, as is commonly accepted, then the phenomenon of the "true" (classical-like) dynamical chaos strictly speaking does not exist in nature. Nevertheless, the conception of "true" chaos is very important in the theory as the limiting pattern to compare with real quantum chaos.

3.4 Dynamical stability of quantum diffusion

Even though quantum diffusion and relaxation proceed on a fairly long time scale (25) they are very unusual and qualitatively different from their classical counterparts, namely they are dynamically stable. This was shown in several numerical experiments with time reversal [23]. Particularly, for the diffusive ionization of the Rydberg hydrogen atom in a microwave field (Fig.6) the electron velocity was reversed at $t = 60$ field periods, and the backward motion was observed. In the

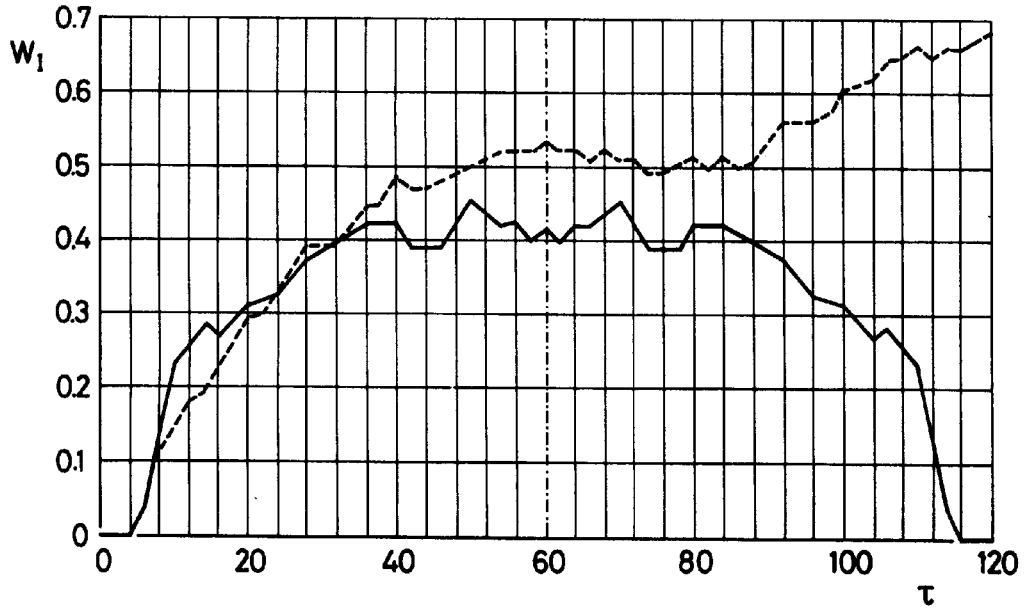

Fig. 6. Classical (dashed curve) and quantum (full curve) ionization probability as a function of time. Notice the perfect symmetry of the quantum curve about the time of reversal ($\tau = 60$ field periods). Both classical and quantal diffusive ionization lag in time which is a characteristic distinction from direct multiphoton ionization. (after Ref.[12]).

classical case the reversed motion reproduces the forward motion for a very short time only because, due to exponential instability, unavoidable computational errors immediately restore the diffusion. Unlike this, in the quantum system the "antidiffusion" goes back to the initial state with very high accuracy ($\sim 10^{-15}$) and only after passing the initial state does the quantum diffusion continue. The stability of quantun chaos over the relaxation time scale is comprehensible since the random time scale is much shorter. Yet, the accuracy of the reversal is surprising. Apparently, this is explained by the relatively large size of the quantum wave packet as compared to the unavoidable rounding-off errors (δ). In the SM, for example, the size of the least-spreading wave packet $\Delta\vartheta \sim \sqrt{T}$. On the other hand, any quantity in the computer must exceed the error δ. Since $T > \delta$, then $(\Delta\vartheta)^2/\delta^2 \sim (T/\delta)\delta^{-1} \gg 1$. This experiment clearly indicates that there is no appreciable instability in quantum chaotic motion. It is also an example which demonstrates that exponential instability is not necessary for a meaningful statistical description. An interesting version of the time-reversal experiment with controlled perturbation, much in excess of rounding-off errors, is described in Ref.[24].

The statistical relaxation to a steady state as described by a diffusion equation is typically exponential, yet this does not mean that the underlying dynamical motion is necessarily unstable as is sometimes assumed [25].

4 The quantum steady state

The quantum statistical relaxation results in the formation of the steady state which crucially depends on the ratio

$$\lambda^2 \sim \frac{\tau_R}{\tau_{cl}} \tag{34}$$

We call λ the *ergodicity parameter*. If $\lambda \gg 1$ then the relaxation time scale is long enough for the system to approach the steady state which is close to the classical ergodic steady state (22). (In a different quantum model behaviour close to the classical one was also observed but misinterpreted [65]). Nevertheless neither the $\psi-$function nor the density matrix are identical to the classical steady state. The essential difference is in finite stationary oscillations in the quantum case due to the discrete spectrum. For example in the SM on the torus the expected fluctuations of the energy $E =< n^2 > /2$ are

$$\frac{\Delta E}{E_s} \sim \frac{1}{\sqrt{L}} \tag{35}$$

where $E_s = L^2/24$ is the average energy on the torus $(-L/2, L/2)$. This would imply that the ψ-function represents a finite ensemble of $\sim L$ systems even though formally it describes a single system. In other words the ψ-function plays an intermediate rôle between the trajectory and the distribution function in classical mechanics. Indeed, $|\psi|^2$ is not a constant like the classical (coarse-grained) distribution function in the steady state but its fluctuations are much smaller than those of a single classical trajectory which would be $\Delta E/E_s \sim 1$.

If $\lambda \ll 1$ the relaxation time scale is insufficient to reach the classical steady state and a qualitatively different quantum steady state is formed. For example, in the SM the steady state distribution in momentum is approximately exponential [26]

$$g_s(n) \sim \exp\left(-\frac{2|n-n_0|}{l_s}\right) \tag{36}$$

This is the well known phenomenon of quantum diffusion localization. Here l_s is called the *localization length*, and a sufficiently narrow initial state $g(n, 0) \sim \delta(n - n_0)$ is assumed. From the diffusion law $l_s^2 \sim D_0\tau_R$ hence from Eq.(27) $l_s \sim D_0$. Numerical experiments confirm this estimate and give the more accurate result [26]

$$l_s \approx D_0 \tag{37}$$

The distribution (36) is completely different from the classical ergodic state and we call it the *quantum steady state*. This state represents a finite ensemble of about l_s systems; hence, as with Eq.(35), we would expect the fluctuations to be of the order $1/\sqrt{l_s} \sim 1/k$. However, numerical experiments show that the

fluctuations are much bigger:

$$\frac{\Delta E}{E_s} \sim k^{-0.6} \tag{38}$$

These are possibly related to the so-called Mott states (see below) [27,59].

Eq.(36) allows the definition of the ergodicity parameter (34) in a more precise way in terms of l_s:

$$\lambda = \frac{l_s}{L} \approx \frac{D_0}{L} \tag{39}$$

The first equality makes sense only for small λ, when the steady-state distribution is exponential (36). At larger $\lambda \gtrsim 1$ the approximate equality in Eq. (39) should be taken. The ratio D_0/L is an important parameter of this model and its relation to the ergodicity will be considered in Section 9.

Numerical experiments [19] show that all eigenfunctions are, on average, also exponentially localized:

$$\varphi_m(n) \sim \exp\left(-\frac{|m-n|}{l}\right) \pm \exp\left(-\frac{|m+n|}{l}\right) \tag{40}$$

where the signs correspond to symmetric and antisymmetric eigenfunctions, respectively, and the localization length is given by

$$l \approx \frac{l_s}{2} \approx \frac{D_0}{2} \tag{41}$$

The two exponential peaks in Eq.(40), separated by a distance of $2|m|$, are due to the exact parity conservation that is to the symmetry with respect to reflection $\vartheta \to -\vartheta$ or $n \to -n$ in the SM.

The difference between the two localization lengths, l and l_s, is due to very big fluctuations around the simple average law (40). This law actually holds asymptotically as $|m \pm n| \to \infty$. Indeed, the central part of each peak in Eq.(40) is not only substantially affected by big fluctuations but may have a very special shape in the case of the so-called Mott states [28] (see also Ref.[18]). These states appear as pairs of approximately symmetric and antisymmetric superposition of the two exponential peaks separated by a distance M (in n) for each of the peaks in Eq.(40). The main characteristic of Mott states is the dependence on M of the quasienergy splitting $\Delta\epsilon$ in the pair. According to numerical experiments [59] this dependence is approximately

$$\Delta\epsilon \approx \frac{0.3}{Tl_s}\left(1 + \frac{M}{l_s}\right)\exp\left(-\frac{M}{l_s}\right) \tag{42}$$

Even though there are only relatively few Mott states they essentially affect the asymptotic relaxation to the quantum steady state [18].

Another definition of the localization length l_H was introduced in Ref.[45]

using the entropy of eigenfunctions

$$l_H = \exp(H); \qquad H = -\sum_{n=1}^{L/2} |\varphi(n)|^2 \ln |\varphi(n)|^2 \tag{43}$$

This definition is especially convenient in the intermediate case where the ergodicity parameter $\lambda \sim 1$ and the eigenfunctions are quite different from the exponential shape (40). The entropy localization length (43) is a particular case of the *Renyi participation ratio* ξ_q which can be defined as (cf. Ref.[30])

$$\frac{1}{\xi_q} = \left(\sum_n |\varphi(n)|^{2q}\right)^{\frac{1}{q-1}} = \langle |\varphi(n)|^{2(q-1)} \rangle^{\frac{1}{q-1}} \tag{44}$$

where q is a continuous parameter. It is easily seen that $l_H = \xi_1$.

For a single exponential peak $\left(|\varphi(n)|^2 = \left(\frac{1}{l}\right) \exp\left(-2|n|/l\right)\right)$ we have:

$$\frac{l}{\xi_q} = \left(\frac{1}{q}\right)^{\frac{1}{q-1}} \to \begin{cases} q & q \ll 1 \\ 1/e & q = 1 \\ 1/2 & q = 2 \\ 1 & q \gg 1 \end{cases} \tag{45}$$

All SM eigenstates are doubly degenerate. If this symmetry is broken by an additional perturbation the localization length, or better to say, the ratio l/D_0, generally rises [34] due to the increase of the number of operative eigenfunctions. However, this effect is generally different for different eigenstates [35].

The fluctuations of l_H for $\lambda \ll 1$, are fairly well described by the following empirical expression for the differential probability [60]

$$p(H) = \frac{1}{\cosh\left[\pi(H - \overline{H})\right]} \tag{46}$$

where $\overline{H}$ is the entropy averaged over all eigenstates. Therefore, unlike the fluctuations of the asymptotic localization length l, the fluctuations of l_H are quite big, namely, the rms $\Delta l_H / l_H \approx 1/2$. No explanation of the simple dependence (46) exists as yet. Notice that l is determined essentially by the tail of the eigenfunction, while l_H is mainly determined by the central part.

Numerical experiments [16] showed that the dimensionless localization length $\beta_{\overline{H}} = \exp\left(\overline{H} - H_e\right) = 2 l_{\overline{H}}(\gamma/L)(\gamma \approx 2)$ depends only on the dimensionless ergodicity parameter λ (39) and not separately on D_0 and L. Here $H_e = \ln(L/2\gamma)$ is the entropy of the ergodic state which is less than maximal ($\ln(L/2)$) because of fluctuations.

The explicit empirical dependence is given approximately by

$$\beta_{\overline{H}} = \begin{cases} \dfrac{\alpha\lambda}{1+\alpha\lambda} & \lambda \le 0.5 \\ 1 - \dfrac{1}{\alpha\sqrt{\lambda}} & \lambda \ge 0.1 \end{cases} \tag{47}$$

with $\alpha \approx 4$.

A partial explanation of the first scaling in Eq.(47) is related to the dependence of any ξ_q on the position of the exponential peak inside the interval $(0, L)$ due to the symmetry of eigenfunctions. Then, averaging over the different eigenvectors we obtain for $\lambda \lesssim 1$

$$\left\langle \frac{1}{\xi_q} \right\rangle \approx \frac{1}{\xi_q(\infty)} + \frac{C_q}{L} \tag{48}$$

where $\xi_q(\infty)$ is the localization length in the limit $L \to \infty$ and where the constant

$$C_q = \sum \left[\frac{1}{\xi_q} - \frac{1}{\xi_q(\infty)} \right] \tag{49}$$

depends on the shape of eigenfunctions, including fluctuations. Relation (48) is equivalent to the first scaling (47) with $C_1 = \gamma$ and $\gamma \xi_1(\infty) = \alpha D_0$. The second scaling (47) has still to be understood.

In the classical limit $\lambda \sim k^2/L = (K/LT)k \sim k \to \infty$ hence all eigenfunctions become ergodic in accordance with the Shnirelman theorem (see below).

An interesting microstructure of chaotic eigenfunctions was discovered by Heller (see Ref.[31]) and was termed "scars". These are enhancements of the density of eigenfunctions along classical periodic orbits in spite of the fact that all these orbits are unstable. A general theory of scars was developed in Refs.[29,32] using a very powerful method of Gutzwiller based on classical periodic orbits. In particular each such orbit determines the corresponding scar, the change of density being proportional to $\exp(-h_p T_p/2)$ where T_p is the orbit period, and $h_p \approx \sum \Lambda_+$ is the sum of positive Lyapunov exponents, the analogue of KS entropy for the unstable periodic orbit. Thus, appreciable scars appear only along the short-period orbits with $T_p \lesssim 1/h_p \approx 1/h$ where h is the classical KS entropy.

At first glance scars contradict the Shnirelman theorem [33] which states, loosely speaking, that classical ergodicity implies ergodicity for most eigenfunctions sufficiently far in the quasiclassical region (see also Refs.[54]). However, this is not the case because the spatial size of scars is minimal (of the order of the elementary quantum cell) while the Shnirelman theorem is of integral type. Indeed, according to Shnirelman the definition of an ergodic eigenfunction W_n (in Wigner's representation) is given by the expression

$$\int dpdq\, W_n(p, q) f(p, q) \underset{n\to\infty}{\longrightarrow} \int dpdq\, g_\mu(p, q) f(p, q) \tag{50}$$

for any sufficiently smooth function f of phase space. Here

$$g_\mu = \delta\,(H(q, p) - E)\,\frac{dE}{dpdq} \tag{51}$$

is the microcanonical measure. The quantity $\rho(E) = dqdp/dE$ is the classical counterpart of the mean level density. The above definition of ergodicity is

insensitive to the microstructure of the eigenfunction. Some eigenfunctions are known to be almost completely localized on a periodic orbit but the proportion of these rapidly decreases as $n \to \infty$ [55].

5 A phenomenological theory of quantum relaxation

In this section we derive a diffusion equation which describes the quantum relaxation process. As is known, in classical statistical mechanics the relaxation process is described by a diffusion equation. The same equation describes the quantum relaxation for $\lambda \gg 1$ when the final steady state is ergodic. However, in the case $\lambda \lesssim 1$ the quantum diffusion leads to a localized, non ergodic, steady state, and therefore it is necessary to modify the classical diffusion equation to include the phenomenon of localization. One way to do this is to use the complete Fokker–Planck equation with the so-called drift term [36]

$$\frac{\partial g}{\partial \tau} = \frac{1}{2}\frac{\partial}{\partial n} D(n) \frac{\partial g}{\partial n} - \frac{\partial}{\partial n} Bg \tag{52}$$

where

$$B = \frac{< \Delta n >}{\tau} - \frac{dD(n)}{dn} \tag{53}$$

In our problem this term describes the so-called backscattering, that is, the reflection of the ψ-wave propagating in n (see Section 6).

For sufficiently short times the diffusion is determined by the first term on the rhs of Eq.(52) and coincides with the classical diffusion. However, as time increases the backscattering eventually suppresses the diffusion and leads to a steady state (36). The general expression for the steady state $g_s(n)$ can be derived from Eq.(52) and is given by

$$\ln g_s = 2 \int \frac{B(n)dn}{D(n)} \tag{54}$$

In the case of homogeneous diffusion where $D = const$, the steady state Green function g_s is given by Eq.(36) with $l_s = D$. Hence, from Eq.(54) we obtain

$$B = \begin{cases} +1 & n < n_0 \\ -1 & n > n_0 \end{cases} \tag{55}$$

where n_0 is the initially excited state. It is remarkable that B turns out to be independent of the system's parameters and this may point to a quite general applicability of the method. Since the backscattering function $B(n)$ depends on the particular initial condition, the diffusion Eq.(52) describes the Green function only, which is initially $g(n, \tau) = \delta(n - n_0)$. Without loss of generality we can take $n_0 = 0$. Due to the symmetry with respect to $n = 0$ we can consider only the region $n > 0$. The diffusion equation then reads

$$\frac{\partial g}{\partial \tau} = \frac{D}{2} \frac{\partial^2 g}{\partial n^2} + \frac{\partial g}{\partial n} \tag{56}$$

with boundary conditions

$$g(\infty, \tau) = 0$$
$$\frac{D}{2}\left(\frac{\partial g}{\partial n}\right)_{n=0} + (g)_{n=0} = 0$$

The solution of Eq.(56) can be found via Laplace transform and in the dimensionless variables $x = n/2D$, $s = \tau/2D$ reads:

$$g(x,s) = \frac{1}{\sqrt{\pi s}} \exp\left[-\frac{(x+s)^2}{s}\right] + \exp(-4x)\,\mathrm{erfc}\left(\frac{x-s}{\sqrt{s}}\right) \tag{57}$$

where

$$\mathrm{erfc}(u) = \frac{2}{\sqrt{\pi}} \int_u^\infty \exp(-v^2)\, dv$$

Initially, all the probability $\left(\int_0^\infty g\,(x,s)\, dx = 1/2\right)$ is in the first term of (57) while asymptotically the whole probability goes in the second term, and for $s \to \infty$ the steady-state distribution is given by

$$g(x) = 2\exp(-4x) \qquad\qquad x > 0 \tag{58}$$

Let us now compute the first two moments $< x >$ and $< x^2 >$. The equations for them are

$$\left.\begin{aligned} \frac{d}{ds} < x > &= \frac{1}{2} g\,(0,s) - 1 \\ \frac{d}{ds} < x^2 > &= \frac{1}{2} - 4 < x > \end{aligned}\right\} \tag{59}$$

which lead to the solution

$$< x >= \frac{1}{4} - \frac{1}{2}\mathrm{erfc}\,(\sqrt{s})\left[\frac{1}{2} + s\right] + \frac{1}{2\sqrt{\pi}}\sqrt{s}\,\exp(-s)$$

$$< x^2 >= \frac{E}{2D^2} = \frac{1}{8} + \frac{1}{2}\mathrm{erfc}\,(\sqrt{s})\left[s + s^2 - \frac{1}{4}\right] - \frac{1}{2\sqrt{\pi}}\sqrt{s}\,\exp(-s)\left(\frac{1}{2} + s\right) \tag{60}$$

From this equation it follows that the relaxation to the steady state value $< x^2 > \to 1/8$ is exponential. This is not in agreement with numerical computations where a power law relaxation was found for sufficiently large s [18]. To explain such a behaviour we need to take into account the explicit time dependence of $D(\tau) = D_0\, d(\tau)$ which follows from the discrete quantum spectrum. Notice that the ratio $D(\tau)/B(\tau)$ must be independent of time, at least asymptotically, to provide the exponential steady state (36). It follows that $B(\tau) = -d(\tau)$ with $d(\tau) \to 1$ as $\tau \to 0$.

As was remarked in Ref.[43] the diffusion rate must be proportional to the number of quasi-energy levels which are not yet resolved in time τ. This number decreases, for $\tau \geq \tau_R$ as $1/\tau$. We may therefore take

$$d(s) = \frac{\alpha}{\alpha + s}$$

where α is some unknown parameter ~ 1. The new solution of the diffusion equation (56), with time-dependent diffusion coefficient, remains the same "$g(x, \sigma)$ in (57)" in a new time variable

$$\sigma = \int d(s)\, ds \to \alpha \ln\left(1 + \frac{s}{\alpha}\right)$$

where now $x = n/2D_0$ and $s = \tau/2D_0$. Notice that the above logarithmic dependence is the only one which provides a power law relaxation in s for $g(x, \sigma(s))$.

Asymptotically, the relaxation goes as $s^{-\alpha}$ $(s \to \infty)$. Comparison with numerical data [18,27] shows that $\alpha \approx 1$ which is also the result of a different theory [18].

From Eq.(60) we may then obtain the asymptotic relaxation law $(s \to \infty)$

$$\frac{E}{D_0^2} \approx \frac{1}{4} - \frac{1}{\sqrt{\pi}\, s\, (\ln s)^{3/2}}; \qquad \frac{dE}{ds} \approx \frac{D_0^2}{\sqrt{\pi}\, s^2\, (\ln s)^{3/2}} \tag{61}$$

while for $s \to 0$ we have

$$\frac{E}{D_0^2} \approx s\left(1 - \frac{8}{3\sqrt{\pi}}\sqrt{s}\right)$$

in agreement with the classical diffusion.

Eq.(61) is close to but not identical with the result in Ref.[18] which, in our notations, reads:

$$\frac{dE}{ds} \approx c\, \frac{D_0^2 \ln s}{s^2} \tag{62}$$

This expression seems to agree quite well with the numerical data in [18] with fitting parameter $c \approx .3$. On the other hand Eq.(60) was also confirmed by numerical data in Ref.[27] for the whole integration time interval. This problem therefore requires further analysis.

Another interesting characteristic of quantum relaxation is the so-called staying probability $g(0, \sigma)$ [30] which is given by

$$g(0, \sigma) = 2 + \frac{\exp(-\sigma)}{\sqrt{\pi\sigma}} - \operatorname{erfc}(\sqrt{\sigma}) \tag{63}$$

and it has the same asymptotic behaviour (61) of the energy

$$g(0, s) \approx 2 + \frac{1}{2\sqrt{\pi}\, s\, (\ln s)^{3/2}} \tag{64}$$

At this point it is necessary to stress that in the SM, where diffusion is homogeneous in n, quantum localization is a universal phenomenon. This is no longer the case when the diffusion rate depends on n. Consider, for example, the case

$$D(n) = D_0\, n^{2\alpha} \tag{65}$$

Then, from Eq.(54) we obtain for the steady state distribution:

$$\ln g_s(n) = \begin{cases} -\dfrac{2n^{1-2\alpha}}{(1-2\alpha)D_0} & \alpha \neq \dfrac{1}{2} \\ -\dfrac{2}{D_0}\ln n & \alpha = \dfrac{1}{2} \end{cases} \tag{66}$$

where we have assumed that $B = -1$ as before since it does not depend on the system's parameters. In agreement with previous results the critical value is $\alpha_c = (1/2)$. For $\alpha < \alpha_c$ the localization remains exponential (as was rigorously shown for a similar solid state model [70]) while for $\alpha > \alpha_c$ delocalization occurs because $g_s(n) \to const \neq 0$ as $n \to \infty$. In the critical case the steady state distribution is a power law

$$g_s \sim n^{-2/D_0} \tag{67}$$

and the localization takes place for $D_0 < 2$ only, when $g_s(n)$ is normalizable.

Notice, however, that unlike the exponential localization, for a power law distribution the conditions of localization depend on the quantity one considers. The above condition $D_0 < 2$ refers to probability localization. However, the energy localization, that is, for the mean energy to be finite in the steady state, a stronger condition is required, namely $2/D_0 - 2 > 1$, or

$$D_0 < \frac{2}{3} \tag{68}$$

which is in good agreement with numerical results, as is shown in Fig.7 [71].

One may also consider the SM (6) with parameter $k(n)$ depending on the dynamical variable n. In this case, however, the map is no longer canonical and in order to obtain the correct description of the global motion, the energy-time dynamical variables should be taken [43] as in the Kepler map (10). As is easily verified the expression for the steady state distribution (54) remain unchanged after appropriate rescaling of both D and B.

A more interesting example is the spin model (14) where the diffusion rate in s_z is given approximately by:

$$D(s_z) = \frac{k_0^2}{2}\left(1 - \frac{s_z^2}{s^2}\right) \tag{69}$$

Consider, for instance, a steady state centred at $s_z = 0$. We have

$$g_s(s_z) \sim \left(\frac{s - |s_z|}{s + |s_z|}\right)^{1/\lambda} \tag{70}$$

where $\lambda = l_0/s$ is the ergodicity parameter, and $l_0 = k_0^2/2$ is the localization length at $s_z \approx 0$. Contrary to the previous understanding [13,14] the diffusion in this model is localized, even for $\lambda \gtrsim 1$, provided $k_0 \ll s$. For a steady state centred at

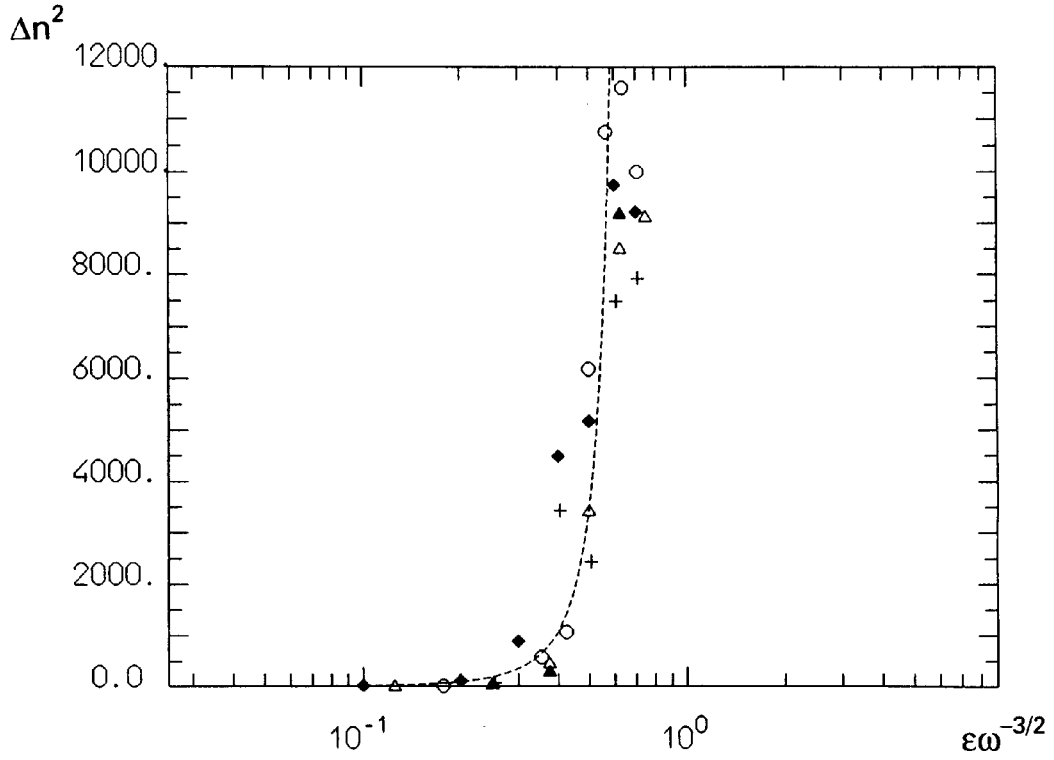

Fig. 7. The spread of the wave packet Δn^2 over the unperturbed states (second moment of the distribution in n), averaged in time from 100 to 200 field periods, vs the decimal logarithm of the variable $\varepsilon\omega^{-3/2}$ for $n_0 = 5$: filled diamonds: $\omega = 1.00$, $\varepsilon_0 = 0.2$; circles: $\omega = 2.00$, $\varepsilon_0 = 1.0$; triangles: $\omega = 2.52$, $\varepsilon_0 = 0.4$; crosses: $\omega = 4.60$, $\varepsilon_0 = 1.44$ and for $n_0 = 10$: filled triangles: $\omega = 2.52$, $\varepsilon_0 = 0.4$. The dashed line is drawn to guide the eye.

the "pole" $s_z = s$ we have

$$g_s(s_z) \sim \left(\frac{s + s_z}{s - s_z}\right)^{1/\lambda} \tag{71}$$

Unlike this, for the motion on hyperboloid (17) the diffusion is always delocalized since for $s_z \gg s$ the situation is the same as in model (65) with $\alpha = 1$.

Consider, finally, the diffusive photoeffect in Rydberg atoms. Instead of using the Kepler map (10) we may solve the problem in the principal quantum number n. Then, the diffusion rate [39] and the backscattering parameter are

$$D_n = \frac{a\varepsilon^2}{\omega^{7/3}} n^3; \qquad B(n) = B(v) \cdot \frac{dn}{dv} \cdot \frac{d\tau}{dt} = B(v) = \pm 1 \tag{72}$$

where t is measured in the number of field periods. From Eq.(54) we thus obtain

$$\ln g_s(n) = -\frac{2\omega^{7/3}}{a\varepsilon^2} |E - E_0| \tag{73}$$

that is an exponential localization in energy with the same localization length as from the Kepler map ($a \approx 3.3$) [12].

The above examples show that the phenomenological theory described in this section gives a reasonable description of the quantum relaxation process. In

particular it would be interesting to check the predictions of Eqs. (70) and (71) numerically.

6 Quantum chaos and Anderson localization

The localization of eigenfunctions for the dynamical problem is similar to the celebrated Anderson localization in disordered solids [72,74]. For the latter problem, of particular interest are the so-called tight binding models which are lattice discretizations of the Schrödinger equation. These models play an important rôle in the investigation of transport properties of solids at low temperature, where the electron wave function becomes very sensitive to local impurities and imperfections of the crystal lattice.

The simplest well-known example is the Lloyd model which is described by the eigenvalue equation:

$$(Hu)_n = u_{n+1} + V_n u_n + u_{n-1} = E u_n \tag{74}$$

where the Hamiltonian H is a sum of a nearest-neighbour interaction term $(H_0\psi)_n = \psi_{n+1} + \psi_{n-1}$ and a local term describing the interaction energy of the electron with the crystal site $(V\psi)_n = V_n\psi_n$. The boundary conditions are $u_0 = u_{N+1} = 0$ and the potential $\{V_n\}$ is a set of N independent random variables, with the same probability distribution:

$$P_w(V) = \frac{1}{\pi}\frac{W}{V^2 + W^2} \qquad W > 0 \tag{75}$$

It is mathematically proven that the above random model in the large N limit displays exponentially localized eigenfunctions, no matter how small the disorder W; the rate of decay is measured by the smallest Lyapounov exponent γ which may be evaluated by Thouless' formula [74] or by the transfer matrix method [75]. Although γ for a finite N depends on the realization of the disorder, in the limit $N \to \infty$ it converges to a non-random value, the inverse of which is known as *the localization length* ξ_∞.

For the Lloyd model, this quantity can be found analytically:

$$\xi_\infty^{-1} = \gamma = \operatorname{Arcosh}\left[\frac{1}{4}\sqrt{(2+E)^2 + W^2} + \frac{1}{4}\sqrt{(2-E)^2 + W^2}\right] \tag{76}$$

The formal analogy between tight binding models and the quantum kicked rotator was discovered in Ref.[40]. It was shown that the equation for the quasienergies or for the Floquet operator

$$\hat{U}\psi = \exp\left(-ik\cos\hat{\vartheta}\right)\exp\left(-i\frac{T}{2}\hat{n}^2\right)\psi = \exp(-i\varepsilon T)\psi \tag{77}$$

can be written as an eigenvalue problem for a "tight binding model"

$$(W_0 - T_m)\,\bar{u}_m + \sum_r W_r\,\bar{u}_{m+r} = 0 \tag{78}$$

where

$$T_m = \tan\left(\frac{\varepsilon}{2}T - \frac{T}{4}m^2\right), \quad W_r = \frac{1}{2\pi}\int_0^{2\pi} d\vartheta \exp(i r \vartheta) \tan\left(\frac{k}{2}\cos\vartheta\right)$$

and $\bar{u}_r$ is the Fourier coefficient of the expansion of $\bar{\psi}(\vartheta) \simeq \frac{1}{2}[1+\exp(ik\cos\vartheta)]\,\psi(\vartheta)$ in the momentum basis.

Eq.(78) is the eigenvalue equation for an electron in a crystal with site m, site energies T_m and hopping matrix elements W_r. This particular transformation must satisfy the bound $|k\cos\vartheta| < \pi$. This restriction can be avoided at the expense of a more complicated transformation as shown in Ref.[41].

For this particular example in the generic case in which T is an irrational multiple of 4π, the localization of the eigenfunction was proven by several numerical computations. This implies that Anderson localization is also possible in a non-random potential. It should be stressed that in the dynamical case no external random element is introduced since the perturbation is periodic and that localization is related here to quasienergy eigenfunctions and occurs in momentum instead of configuration space.

When $T/4\pi$ is rational it is apparent that the potential becomes periodic, the electron is described by Bloch waves and moves freely in the crystal. This situation corresponds to the so-called quantum resonance in the kicked rotator. Indeed let us observe that the quantum description is endowed with two different periods: the first is explicitly specified by the perturbation, the second is 4π and follows from the peculiarity of the free evolution of having a spectrum given by integers. Naively speaking, the free rotator has energy levels $E_n = n^2/2$ and the photon's energy is $2\pi/T$; the resonance condition is met whenever an integer number of photons matches the energy for a transition between unperturbed levels. This condition corresponds to rationality of the ratio $T/4\pi$ between the two periods.

The general *resonant case* $T/4\pi = p/q$ has been investigated by Izrailev and Shepelyansky [62]. In this case the search for quasienergies is reducible to the problem of diagonalizing a $q \times q$ unitary matrix. In fact, they obtained the following Floquet map depending on the parameter θ

$$\psi\left(\vartheta + \frac{2\pi}{q}m\right) = \sum_{n=0}^{q-1} S^{\theta}_{mn}\psi\left(\theta + \frac{2\pi}{q}n\right)$$

$$S^{\theta}_{rs} = \exp[-ik\cos(\theta + 2\pi r/q)]\frac{1}{q}\sum_{m=0}^{q-1}\exp\left[-2\pi i\left(\frac{p}{q}m^2 + m\frac{s-r}{q}\right)\right] \qquad (79)$$

The eigenvalues $\exp[i\lambda_j(\theta)]$ of the unitary matrix S^{θ} have a continuous dependence on the angle $\theta \in [0, 2\pi/q]$, and the spectrum of the resonant Floquet operator is therefore continuous with q bands.

The introduction of a second, incommensurate perturbing frequency in the

kicked rotator produces a sharp increase in the localization length, which grows exponentially with the classical diffusion rate [79]. Again, this is in agreement with the theory of localization in two-dimensional disordered lattices [80].

Since new, incommensurate frequencies in the time-dependent problem introduce new dimensions in the extended phase space, a time-dependent model with three incommensurate frequencies is expected to correspond to a three-dimensional lattice problem, where a transition from localized to extended states occurs at some critical parameter value. Such a transition has indeed been observed [81] and by analysing it, some indications were obtained that may be helpful in clarifying the nature of the Anderson transition itself, which is still in discussion in solid-state physics. In this connection, we wish to emphasize that the one-dimensional character of our time-dependent model allows for a sharp reduction of the computation time needed to analyse the transition, so that recourse to scaling assumptions can be avoided [80].

Let us consider in general the following time-dependent Hamiltonian:

$$H = H_0 + V(\theta, t) \sum_{s=-\infty}^{+\infty} \delta(t - s) \tag{80}$$

The second term describes kicks occurring periodically in time with period one. The free evolution between kicks is given by the Hamiltonian H_0:

$$H_0|n\rangle = E_n|n\rangle, \qquad |n\rangle = \exp(in\theta)/(2\pi)^{1/2} \tag{81}$$

We assume the eigenvalues E_n to be random numbers uniformly distributed in $(0, 2\pi)$. Unlike for the usual kicked rotator, we also assume V to depend explicitly on time according to

$$V \equiv V(\theta, \theta_1 + \omega_1 t, \theta_2 + \omega_2 t) \tag{82}$$

where V is a periodic function of its three arguments to be specified later, and θ_1 and θ_2 are arbitrarily prescribed phases. We would like ω_1 and ω_2 to be incommensurate with each other and also with the frequency of the kicks. Therefore, we take $\omega_1 = 2\pi\lambda^{-1}$ and $\omega_2 = 2\pi\lambda^{-2}$, with $\lambda = 1.3247\cdots$ the real root of the cubic equation $\lambda^3 - \lambda - 1 = 0$. With this choice, ω_1 and ω_2 are a "most incommensurate" pair of numbers. Thus (80) describes the motion of a rotator subjected to periodic kicks, the strength of which is modulated in time by the frequencies ω_1 and ω_2.

The evolution of this rotator, from just after one kick to just after the next, is given by

$$\psi(\theta, t + 1) = \exp[-iV(\theta, t + 1)] \exp(-iH_0)\psi(\theta, t) \tag{83}$$

This formulation of the rotator dynamics is very convenient for numerical simulations because the time dependence of V is known explicitly. Nevertheless, in order to elucidate the connection of this time-dependent problem with a three-dimensional tight-binding model, we must resort to a different formulation as

follows. First of all, we consider the phases θ_1 and θ_2 as new dynamical variables, with conjugate momenta n_1 and n_2. Then we consider the Hamiltonian

$$H' = H_0(\hat{n}) + \omega_1\hat{n}_1 + \omega_2\hat{n}_2 + V(\theta,\theta_1,\theta_2)\sum_{s=-\infty}^{+\infty}\delta(t-s) \tag{84}$$

with $\hat{n}_{1,2} = -i\partial/\partial\theta_{1,2}$. Eq.(84) describes a quantum rotator with three freedoms $(\theta,\theta_1,\theta_2)$ subjected to periodic kicks, the strength of which is not explicitly time-dependent. The one-period propagator for this rotator is the unitary operator

$$\exp[-iV(\theta,\theta_1,\theta_2)]\exp\{-i[H_0(\hat{n}) + \omega_1\hat{n}_1 + \omega_2\hat{n}_2]\}$$

In order to show that the three-dimensional quantum model defined by (84) and the one-dimensional model defined by (80) and (82) are substantially equivalent, we rewrite the Schrödinger equation for the three-dimensional model

$$i\frac{d}{dt}\psi(\theta,\theta_1,\theta_2,t) = H'\psi(\theta,\theta_1,\theta_2,t)$$

in the interaction representation defined by

$$\psi(\theta,\theta_1,\theta_2,t) = \exp[-i(\omega_1\hat{n}_1 + \omega_2\hat{n}_2)t]\tilde{\psi}(\theta,\theta_1,\theta_2,t)$$

In this way we obtain

$$i\,d\tilde{\psi}/dt = H_0\tilde{\psi} + V(\theta,\theta_1+\omega_1 t,\theta_2+\omega_2 t)\sum_{s=-\infty}^{+\infty}\delta(t-s)\tilde{\psi}$$

i.e., the Schrödinger equation for the evolution of the one-dimensional model.

Then, as shown above, the problem of determining the quasienergy eigenvalues and eigenvectors turns out to be formally equivalent to solving the equation

$$T_{\mathbf{n}}\,u_{\mathbf{n}} + \sum_{\mathbf{r}\neq 0} W_{\mathbf{r}}u_{\mathbf{n}+\mathbf{r}} = \epsilon u_{\mathbf{n}} \tag{85}$$

where $\mathbf{n} \equiv (n, n_1, n_2)$ and $\mathbf{r}$ label sites in a three-dimensional lattice,

$$T_{\mathbf{n}} = -\tan\left[\frac{1}{2}\left(E_n + n_1\omega_1 + n_2\omega_2 + \lambda\right)\right]$$

Here λ is the quasi-energy, $W_{\mathbf{r}}$ are the coefficients of a threefold Fourier expansion of $\tan\left[\frac{1}{2}V(\theta,\theta_1,\theta_2)\right]$, and $\epsilon = -W_0$.

We now chose

$$V(\theta,\theta_1,\theta_2) = -2\tan^{-1}\left[2k\left(\cos\theta + \cos\theta_1 + \cos\theta_2\right)\right]$$

so that (85) becomes (compare with Eq.(78))

$$T_{\mathbf{n}}u_{\mathbf{n}} + k\sum_{\mathbf{r}}{}' u_{\mathbf{r}} = 0 \tag{86}$$

where the sum $\sum'$ includes only the nearest neighbours to $\mathbf{n}$. The tight-binding model (86) with the potential $T_{\mathbf{n}}$ is in a sense equivalent to the original rotator

problem. The quasienergy eigenfunctions of the rotator will be localized or extended over the unperturbed eigenstates of H_0 depending on whether the tight-binding model has localized or extended eigenstates; in the localized case, the localization length will be the same. Since the dynamics of the rotator is determined by the nature of its quasienergy eigenstates, any change from localized to extended states that may take place in the tightbinding model (86), as the coupling parameter k is increased, will be mirrored by a simultaneous change in the rotator dynamics, from a localized recurrent behaviour to an unbounded spreading over the unperturbed base. As we mentioned above, the latter type of transition can be numerically detected with less effort than directly tackling the three-dimensional tight-binding model.

The model was investigated by numerical simulation of the quantum dynamics defined by (80) with phases $\theta_1 = \theta_2 = 0$. A transition between two different types of motion was observed around a value $k_{cr} \approx 0.47$, with localization occurring for $k < k_{cr}$ and unbounded diffusion taking place for $k > k_{cr}$.

The dependence of the diffusion rate $D = \langle (n - n_0)^2 \rangle / t$ (in the delocalized regime) and of the inverse localization length $\gamma = l^{-1}$ (in the localized regime) on the perturbation parameter k is shown in Fig. 8. The dependences of D and γ near k_{cr} are consistent with power laws, $D \sim D_0(k - k)_{cr}^s$, $\gamma \sim \gamma_0 (k - k_{cr})^v$ with $D_0 \sim 2.5$, $k_{cr} \approx 0.46$, and $s \approx 1.25$. An analogous fit for the dependence of γ gave $\gamma_0 \sim 3.5$, $k_{cr} \approx 0.469$, and $v \approx 1.5$. Thus the two fittings give very close values of k_{cr} consistent with renormalization theory predictions [78].

The fruitful analogy between Anderson localization and the dynamical problem is extensively used to share various methods and some results in both fields [76,77]. One of the important implications of this analogy is that a random potential is only a sufficient but not a necessary condition for Anderson localization. Hence a new problem arises: the localization in regular (but, of course, not periodic) solids.

One should bear in mind however that this analogy is restricted to the eigenfunctions only. For example the time evolution of a given initial state may be completely different in both problems. In particular, in one-dimensional disordered solids there is no diffusion stage [42] so that Anderson localization is the localization of the free spreading of the initial state. This is immediately seen from the same uncertainity principle which gives the following density of the operative eigenstates

$$\rho_0 \sim \frac{l\, dp}{dE} \sim \frac{l}{u} \tag{87}$$

This is just the localization (relaxation) time scale which is always of the order of the time interval for a free spreading of the initial wave packet at a characteristic velocity u. Thus, only backscattering remains, and its picture is expecially simple, being the interference of scattered waves from different parts of the potential.

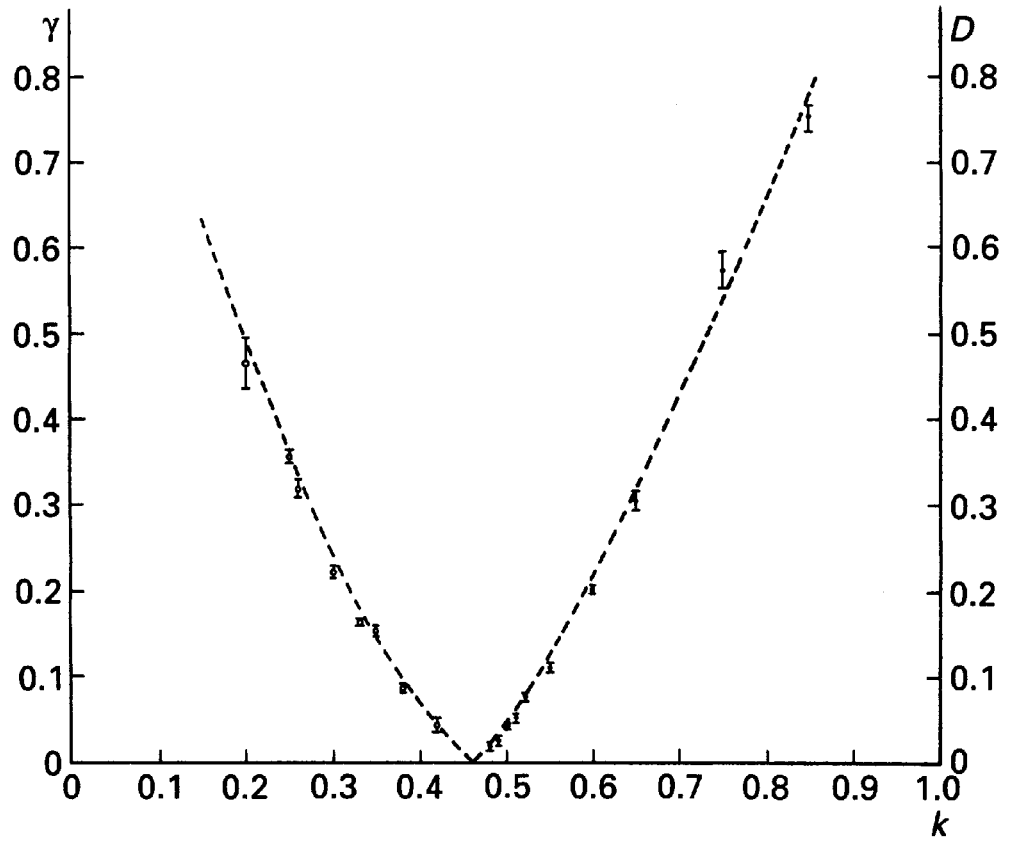

Fig. 8. Diffusion rate D (dots) and inverse localization length $\gamma = 1/l$ (circles) as a function of perturbation parameter k. Error bars were obtained from statistics over ten different realizations of the random spectrum. The dotted lines result from a three parameters least-squares fit of numerical data.

The reason why this general very complicated interference always gives an average backward flow is related to the fact that in a random (or sufficiently irregular) potential there is always a resonant harmonic which provides the complete reflection of the incoming wave. From this explanation it may seem that for localization one needs potentials with continuous spectra. However, this would only be true for an infinitely small amplitude of potential variation. For a finite amplitude the Schrödinger equation in periodic potential is the Mathieu equation with finite instability zones which almost overlap for a sufficiently large amplitude. However, in a periodic potential there are no solutions which would decay in both directions and hence localization is impossible. One needs at least two different periods in the potential to construct a solution decaying in both senses. This would not be universal localization because the instability zones overlap only for sufficiently strong amplitudes. Our conjecture is that the same is true for any discrete spectrum of the potential. Another plausible conjecture is that a continuous spectrum of the potential is a necessary condition for universal localization. However, it may not be sufficient as the interesting example in [73] demonstrates.

7 Experimental observation of localization: the hydrogen atom in a microwave field

One of the most significant cases where classical and quantum chaos confronted each other was in the explanation of an experiment on hydrogen atoms, first performed in 1974 by Bayfield and Koch [82]. Single atoms prepared in very elongated states with a high principal quantum number ($n_0 \approx 63 - 69$) were injected into a microwave cavity and the ionization rate was measured. The microwave frequency was 9.9 GHz, corresponding to a photon energy well below the ionization energy of level 66 and even lower than the transition from state 66 to 67. Much surprise therefore followed the discovery that a very efficient ionization occurred when the electric field intensity exceeded a threshold value of about 20 V per cm (for $n_0 = 66$), much lower than the static Stark value. More surprisingly, a numerical simulation by Leopold and Percival [83] showed that classical mechanics could reproduce the experimental data quite well. The subsequent analysis [39,85], still in classical terms, explained the threshold intensities as critical values for the onset of chaotic diffusion in action space. A condition for the occurrence of full chaotic diffusion is that the microwave frequency is greater than the frequency of the electron's motion, namely $\omega n_0^3 > 1$. However, the hydrogen atom is a quantum object. The quantum mechanical evolution was investigated in the one-dimensional approximation [86] and for $\omega n_0^3 > 1$ it was predicted an ionization threshold higher than the classical value, to overcome the occurrence of quantum localization. This effect vanishes when approaching the main resonant region $\omega n_0^3 \approx 1$, and this may explain why classical mechanics works so well at lower values of ωn_0^3.

The classical Hamiltonian for a one-dimensional hydrogen atom interacting with a time-periodic microwave field in the dipole approximation is

$$H(x', p', t') = \frac{p'^2}{2m} - \frac{e^2}{z'} + eE_0 z' \cos(\omega' t') \qquad z' \geq 0$$

One goes to natural atomic units by setting $z' = z a_0$, where $a_0 = \hbar^2/me^2$ is the Bohr radius, and $t' = tT_0$, where $T_0 = \hbar^3/me^2$. Defining the rescaled parameters $\epsilon = E_0 a_0^2/e$ and $\omega = \omega' T_0$, the dimensionless Hamiltonian is (cf. Eq.(9))

$$H(z, p, t,) = \frac{p^2}{2} - \frac{1}{z} + \epsilon z \cos(\omega t) \tag{88}$$

the energy being measured in units of e^2/a_0. The unperturbed Hamiltonian describes both bounded (with negative energy) and unbounded motions; since we are interested in exploring the dynamics that precedes ionization, we are confined to negative energies, and accordingly introduce action-angle variables (n, θ) thus obtaining Eq.(9).

In the time-independent formalism, the Hamiltonian (9) is replaced by

$$\mathscr{H}(n, \theta, v, \phi) = -\frac{1}{2n^2} + \omega v + \epsilon z(n, \theta) \sin\phi \tag{89}$$

where $\phi = \omega t$ and v is the canonical momentum. Their variations in the auxiliary time η are given by $d\phi/d\eta = \omega$, implying $\eta = t + const$ and $dv/d\eta = -\epsilon z(I, \theta)\cos\phi$. Since $\mathscr{H}$ is a constant of motion, to zero order in ϵ one may view the variation of v as the number of photons exchanged by the atom with the field. We now want to write an approximate map for the canonical variables (v, ϕ). The equations are first integrated over one period of the unperturbed orbit, to first order in ϵ:

$$\left.\begin{aligned} \overline{v} &= v + k\sin\phi \\ \overline{\phi} &= \phi + 2\pi\omega n^3 \end{aligned}\right\} \tag{90}$$

where $k \approx 2.6\,\varepsilon/\omega^{5/3}$ (see eqs.(11) and (13)).

To remove the unwanted n-dependence, one may set from Eq.(89) $n \approx (2\omega v - 4\mathscr{H})^{-1/2}$ and replace v with $\overline{v}$. The resulting canonical map is Kepler's map.

$$\left.\begin{aligned} \overline{v} &= v + k\sin\phi \\ \overline{\phi} &= \phi + 2\pi\omega(2\omega\overline{v} - 2\mathscr{H})^{-3/2} \end{aligned}\right\} \tag{91}$$

which coincides with Eq.(10) after setting the motion integral $\mathscr{H} = 0$. A linearization around the initial value $v_0 = v(n_0)$ and a phase shift, yield once again the SM:

$$\left.\begin{aligned} \overline{v} &= v + k\sin\phi \\ \overline{\phi} &= \phi + T\overline{v} \end{aligned}\right\} \tag{92}$$

with $T = 6\pi\omega^2 n_0^5$. The actual value of v_0 is arbitrary, and reflects the arbitrariness in choosing the zero energy in (89). We decide to take $v_0 = 0$, corresponding to the initial value n_0. The relation between the action and the number of photons is therefore

$$v\omega = \frac{1}{2n_0^2} - \frac{1}{2n^2}$$

In spite of the various simplifications introduced so far, the map (92) still gives a good description of the mean behaviour of the system and allows some conclusions.

The condition $kT \approx 1$ gives the threshold for transition to classical chaos leading to fast ionization.

$$\epsilon_c \approx \frac{1}{50\, n_0^5\, \omega^{1/3}} \tag{93}$$

In the corresponding quantum model we expect, similarly to the kicked rotator, localization of the wave function in v. After the relaxation time τ_R the system reaches the steady state (cf. Eq.(36))

$$g(v) \approx \frac{1}{l_s}\exp\left(-2\frac{|v|}{l_s}\right) \tag{94}$$

The predicted localization length in the number of photons is

$$l_s \approx \frac{k^2}{2} \approx 3.3\epsilon^2\omega^{-10/3}$$

and equals the diffusion coefficient in v-space. If l_s is greater than the number of photons required to ionize the atom $l_s \geq (2\omega n_0^2)^{-1}$, then localization cannot prevent ionization. This takes place for field intensities greater than the *quantum delocalization border*

$$\epsilon_q \approx 0.4\omega^{7/6}n_0^{-1} \tag{95}$$

Unexpected though these predictions may have been at their first appearance [12,86,87], they were confirmed by recent experimental results on the microwave ionization of hydrogen atoms [89, 90]. It was found that experimental and numerical data agree fairly well with localization theory and at the same time appreciably deviate from classical predictions. The experiments described in [90] were designed precisely for the purpose of checking localization theory; as a matter of fact, special care was taken in order that numerical computations could simulate as closely as possible the experimental conditions. Therefore, they provide experimental evidence of the quantum suppression of classically chaotic diffusion due to the localization phenomenon.

In Fig. 9 a comparison of the theory with the experimental data obtained in [89] is presented. The circles represent the experimentally observed threshold values of the microwave peak-field intensity for 10% ionization. Here the microwave frequency $\omega/2\pi = 36.02$ GHz, $\epsilon_0 = \epsilon n_0^4$ is the rescaled peak field intensity, $\omega_0 = \omega n_0^3$ is the rescaled microwave frequency and n_0 is the principal quantum number of the initially excited state value. Both in the experiment and in the quantum numerical computations the ionization probability is defined as the total probability above a cutoff level n_c. The dotted curve is the classical chaos border and the dashed curve in Fig. 9 is the theoretical prediction of localization theory for the 10% threshold value. Unlike the previous case of Ref. [90], the numerical data here were obtained from the numerical simulations of the "quantum Kepler map". In such simulations the interaction time, including the switching on and off of the microwave field, was chosen to be the same as in actual experiments.

The agreement between experimental and numerical data is the more remarkable, in that the quantum Kepler map is only a crude approximation for the actual quantum dynamics. In particular, from Fig. 9 it is seen that when the principal quantum number n_0 of the initial state is increased the data follow the predictions of localization theory.

Though the numerical model was one-dimensional, in actual experiments the initially excited state corresponds to a microcanonical distribution over the shell with a given principal quantum number. The classical counterpart for this would be a microcanonical ensemble of orbits. Nevertheless, the experimental data agree fairly well with the predictions of the one-dimensional quantum Kepler

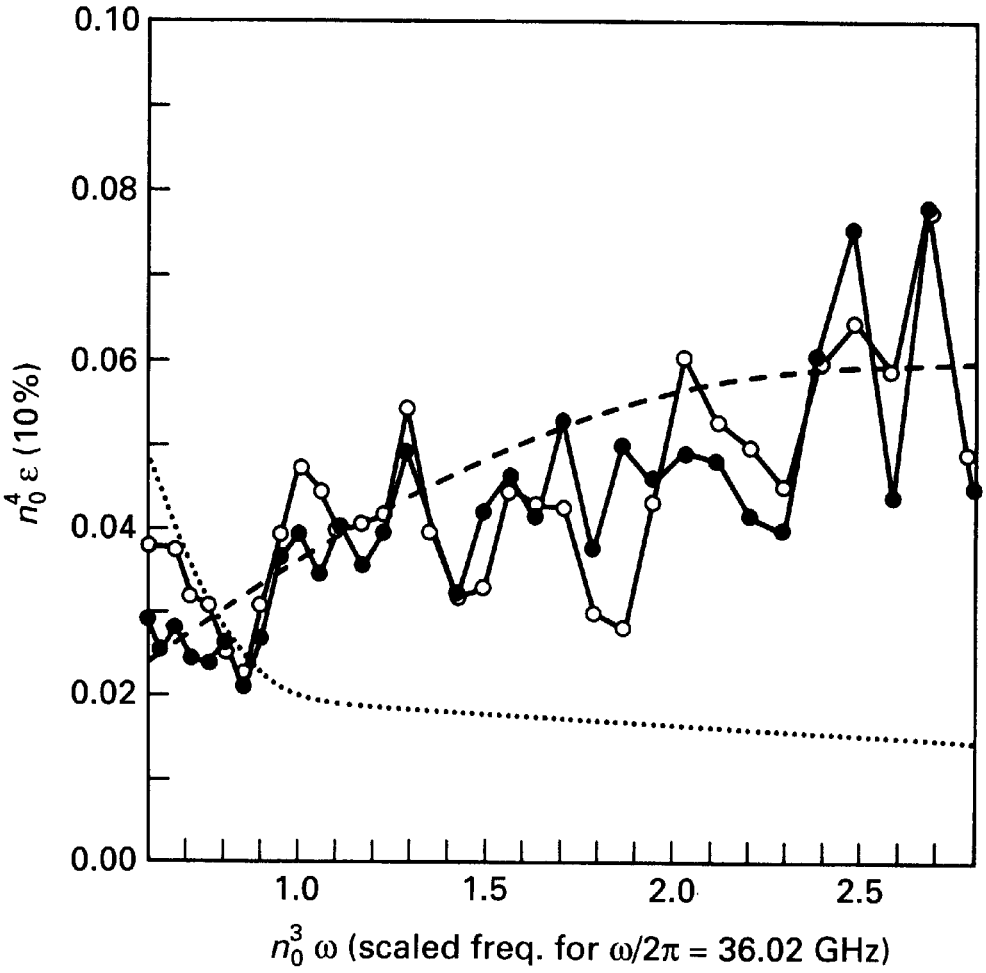

Fig. 9. Scaled 10% threshold fields from experimental results (taken from Fig. 2a, Ref.[89]), (circles), and from numerical integration of the quantum Kepler map (full circles). Curves have been drawn to guide the eye. The dashed line is the quantum theoretical prediction according to localization theory. The dotted curve is the classical chaos border (from Ref.[77]).

map. The reason for this agreement was found in Ref. [12]: due to the existence of an approximate integral of the motion, the main contribution to excitation turns out to be given by orbits which are extended along the direction of the (linearly polarized) external field. For such orbits, the use of the one-dimensional model is fully justified (see, e.g., Fig. 18b in Ref. [12]). Moreover, by using the Kepler map formulation, it has been theoretically and numerically shown [88] that the introduction of a second incommensurate frequency leads to a significant decrease of the threshold border for ionization. It would be interesting to have an experimental confirmation of this prediction.

In closing this section we would like to mention a new feature of this problem which is currently under investigation. Namely it has been shown recently [84] that, at field amplitudes much larger than the classical chaos border, the classical ionization probability *decreases* with *increasing* field intensity. This effect should be observable in laboratory experiments.

8 Fractal spectrum and anomalous diffusion

For motion bounded in phase space the quantum spectrum is always discrete as for example in the kicked rotator on a torus where the spectrum consists of L lines. For unbounded motion the spectrum has, generally, a very complicated structure, even for such a simple model as the SM on the cylinder. This problem has as yet no rigorous solution. In the QSM the spectrum is known to be continuous if the parameter $T/4\pi = r/q$ is any rational number other than $\frac{1}{2}$. Notice that such a spectrum does not mean any chaotic motion but corresponds to a peculiar process which is called *quantum resonance* since the quantity $T/4\pi$ is the ratio between the unperturbed and driving frequencies [11, 62]. In quantum resonance (which has no classical counterpart) the momentum n grows, on average, proportionally with time and hence the energy $E \sim \tau^2$. Using the analogy with the solid state problem described above quantum resonance corresponds to the free motion of the electron (quantum particle) in an exactly periodic potential (the so-called Bloch states).

Quantum resonance is a peculiarity of the kicked rotator model, which is periodic in n. Even though the resonant values of $T/4\pi$ have zero measure they are everywhere dense and this leads to difficulties in the analysis of the *typical* dynamics of this model when $T/4\pi$ is irrational. The resolution of this difficulty is in that the rate of the resonant motion (E/τ^2) rapidly decreases as the denominator q increases. This is approximately described by the semiempirical expression

$$< n^2 > \approx D\,\tau^2 \exp\left(-\frac{2q}{D}\right) \tag{96}$$

which is valid for $q \gtrsim D$.

A detuning from resonance $\epsilon(q) = | T/4\pi - r/q |$ would stop the growth after a time $\tau(\epsilon)$ which, on account of Eq.(23), can be assumed to be

$$\epsilon \tau n^2 = \nu \sim 1 \tag{97}$$

Consider now the irrational

$$\frac{T}{4\pi} = (m_1, m_2 \cdots m_i, \cdots) \equiv \cfrac{1}{m_i + \cfrac{1}{m_2 + \cdots}} \tag{98}$$

in the continued-fraction representation, and its convergents r_i/q_i

$$r_i/q_i = (m_1, \cdots m_i) \to \frac{T}{4\pi} \quad ; \qquad q_{i+1} = m_{i+1}\, q_i + q_{i-1}$$

Our aim is to identify the set of irrationals $T/4\pi$ for which a growth law of the form

$$< n^2 > = G\,\tau^{\delta} \tag{99}$$

occurs for any $G > 0$ and δ in the interval (0, 2). To this end we substitute (99) in (97) and after eliminating τ with Eq.(96) we have

$$\epsilon(q_i) = \frac{v}{G}\left(\frac{D}{G}\right)^{\frac{1+\delta}{2-\delta}} \exp\left(\frac{-2q_i}{D}\frac{1+\delta}{2-\delta}\right) \tag{100}$$

On the other hand from the continued-fraction representation of $T/4\pi$ we have

$$\epsilon(q_i) \approx \frac{c}{q_i q_{i+1}} \tag{101}$$

with $c \sim 1$. Then, from (100) and (101) we obtain the relation which allows the construction of the irrational values of $T/4\pi$ giving the desired growth rate (99) and therefore the continuous spectrum

$$m_{i+1} \approx \frac{q_{i+1}}{q_i} \approx \frac{c\,G}{v\,q_i^2}\left(\frac{G}{D}\right)^{\frac{1+\delta}{2-\delta}} \exp\left(\frac{2q_i}{D}\frac{1+\delta}{2-\delta}\right) \tag{102}$$

In the whole interval $0 < \delta < 2$ the motion is unbounded and the spectrum is singular continuous with a fractal structure. The maximal allowed value $\delta = 2$ corresponds to the resonant values of $T/4\pi$ for which the spectrum is absolutely continuous. We would like to attract the reader's attention to the fact that Eq.(102) leads (for $\delta > 0$) to the irrationals that are approximated by rationals to exponential accuracy (the so-called Liouville, or transcendental, numbers) in agreement with known rigorous results [44] which prove the existence of the irrationals $T/4\pi$ leading to a continuous spectrum and unbounded energy growth. However, from the above discussion a new conclusion can be drawn, namely, that even inside those transcendental values of $T/4\pi$ there are infinitely many such ones which lead to localization. They correspond to $\delta = 0$ with finite G. This implies localization for typical irrationals. From Eq.(102) with $\delta = 0$ we can derive the asymptotic condition for the set of irrationals leading to localization:

$$m_i < \exp\left(\frac{q_i}{D}\right) \tag{103}$$

Therefore in the case of a quantum kicked rotator, dynamical localization takes place for almost all irrational values of the ratio between the unperturbed and external frequencies. Correspondingly the spectrum has a pure point character. The band structure obtained by approaching the irrational value via a sequence of rational approximants is characterized by bandwidths which shrink exponentially with respect to the number of bands and this excludes the possibility of self-similarity.

However, fractal features of the spectrum with a corresponding rich variety of dynamical behaviour have been shown to appear in an interesting model, the so-called kicked Harper model which is obtained by quantizing the following

area-preserving map [94]

$$\left.\begin{aligned} p_{n+1} &= p_n + K \sin x_n \\ x_{n+1} &= x_n - L \sin p_n \end{aligned}\right\} \tag{104}$$

In particular this model describes the motion of electrons in two-dimensional lattices in the presence of a magnetic field and can lead to a better understanding of the physics of such systems.

The classical map (104) is known to be chaotic for $KL \gtrsim 1$. As in the case of the kicked rotator, the quantum motion is governed by the one-period evolution operator

$$\hat{U} = \exp\left[-i\left(\frac{L}{\hbar}\right)\cos(\hbar\hat{n})\right]\exp\left[-i\left(\frac{K}{\hbar}\right)\cos x\right] \tag{105}$$

where $\hat{n} = -i\dfrac{d}{dx}$.

Quantum motion has been studied for a strongly irrational value $\hbar = 2\pi/(m + \rho_{GM})$ with $\rho_{GM} = (\sqrt{5}+1)/2$. Approaching this value via a sequence of rational convergents $\{p_n/q_n\}$ (by successive truncations of the continued fraction expansion of $\hbar/2\pi$) one obtains, at each convergent, a band spectrum with Bloch eigenfunctions. Analysis of the spectrum shows that regular scaling behaviour coexists with irregular scaling [91]. Moreover, the dynamical behaviour shows anomalous diffusion $< \Delta n^2(t) > \sim t^{\alpha}$ where the exponent $0 \leq \alpha \leq 2$ depends on the parameters K and L (Fig. 10(*a*)) [92]. This anomalous diffusion builds up at sufficiently large times while initially the diffusion is always close to the classical one ($\alpha = 1$) in accordance with correspondence principle (see Fig. 10(*b*)).

In conclusion the structure of the quasienergy spectrum and the quantum motion of classically chaotic systems appear to be much more rich than previously expected. While for the KR problem this complex structure is confined to a set of zero measure, for the kicked Harper model it appears to be the generic case. In spite of the progress made in the last 15 years the above results indicate that we are still far even from a qualitatively clear understanding of the quantum motion of classically chaotic systems and, moreover, a rigorous mathematical analysis appears to be more and more difficult.

There are also examples of the "true" chaos in quantum mechanics which have the strongest statistical property – the exponential instability of motion for the infinite time interval. One particular model is the following: consider a classical dynamical system on a N-dimensional torus specified by the equations:

$$\dot{\vartheta}_i = \omega_i(\vartheta_k) \qquad i, k, = 1, 2, \cdots N \tag{106}$$

If $N \geq 3$ classical chaos is possible with exponentially unstable solutions of the linearized equations.

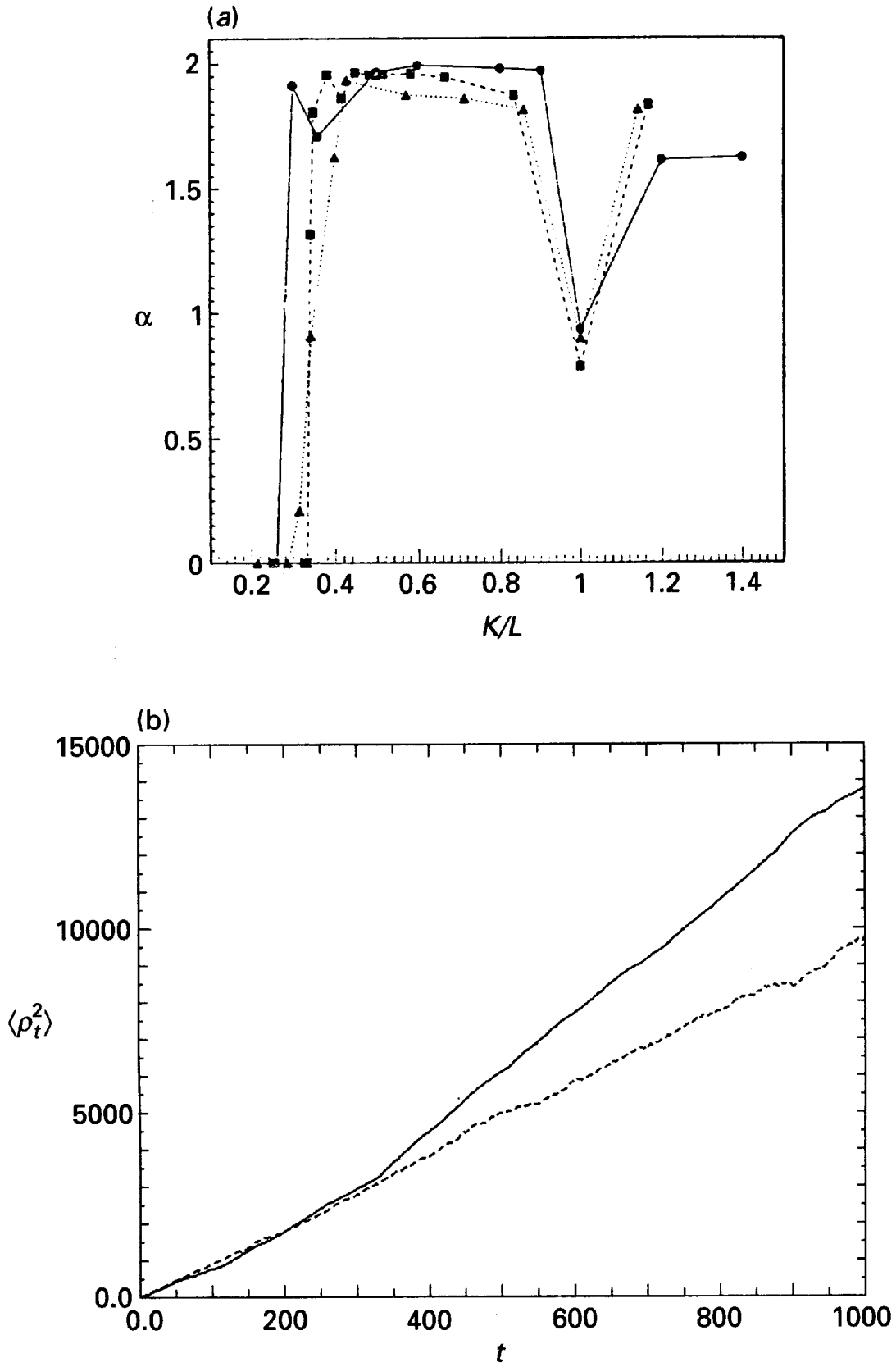

Fig. 10. (*a*) Dynamical exponent α vs K/L for some fixed values of L. Circles are for $L = 5$ and $1.3 < K < 7$, squares for $L = 6$ and $1.5 < K < 7$, triangles for $L = 7$ and $1.5 < K < 8$. Notice the minimum corresponding to the critical line ($K = L$). Each α was determined by examining a time series up to 3 x 10^4 kicks. (*b*) Example of anomalous quantum diffusion (solid line) for $K = L = 5$ and $\hbar = 2\pi/(18 + q_{GM})$, compared with classical diffusion (dotted line) for the same $K = L = 5$. Notice that the quantum diffusion is close to the classical up to a finite time (which increases as $\hbar \to 0$).

One particular example due to Arnold is

$$\left.\begin{aligned}\dot{\vartheta}_1 &= cos\ \vartheta_2 + sin\ \vartheta_3\\ \dot{\vartheta}_2 &= cos\ \vartheta_3 + sin\ \vartheta_1\\ \dot{\vartheta}_3 &= cos\ \vartheta_1 + sin\ \vartheta_2\end{aligned}\right\} \tag{107}$$

Consider the Hamiltonian

$$H(n, \vartheta) = \sum_{1^k}^{3} n_k\ \omega_k\ (\vartheta) \tag{108}$$

The equations of motion are

$$\left.\begin{aligned}\dot{\vartheta}_i &= \omega_i(\vartheta)\\ \dot{n}_i &= -\textstyle\sum_k n_k \dfrac{\partial \omega_k}{\partial \vartheta_i}\end{aligned}\right\} \tag{109}$$

The equations for the momenta coincide (apart from a time-reversal) with the linearized equations of system (106). Therefore if system (106) is chaotic and time-reversible (like example (107)), then the momenta in (109) grow exponentially with time.

Consider now the quantized version of system (108)

$$\hat{H} = \frac{1}{2}\sum_{1^k}^{s}(\omega_k\,\hat{n}_k + \hat{n}_k\,\omega_k); \qquad \hat{n}_k = -i\frac{\partial}{\partial \vartheta_k} \tag{110}$$

From the Schrödinger equation we obtain, for the quantum probability density $f(\vartheta, t) = |\psi(\vartheta, t)|^2$:

$$\frac{\partial f}{\partial t} + \sum_k \frac{\partial}{\partial \vartheta_k}(f\,\omega_k) = 0 \tag{111}$$

This equation exactly coincides with the continuity equation of the classical system (106) and therefore, the quantum probability evolves in time exactly like the probability of the classical chaotic motion.

Even though the above, and other similar examples, are quite exotic, they are very useful for understanding the nature of quantum chaos. A common feature of these examples is that, in order to have the "true" quantum chaos, the momenta must grow exponentially with time. Indeed, as we stated in the introduction, the exact (not coarse-grained) classical distribution function does not approach a homogeneous distribution even in the case of chaotic motion. On the contrary, it becomes more and more scarred due to the local instability of motion and, correspondingly, the wave numbers of the Fourier harmonics grow exponentially. In quantum mechanics this corresponds to an exponential growth of momenta. Notice, however, that even in these exotic examples the true quantum chaos is restricted to configurational space only. (For further discussion of such examples see Ref.[56].)

9 Quantum chaos and the random matrix theory

The complete solution of the dynamical quantum problem is given by the diagonalization of the Hamiltonian to find the energy (or quasienergy) eigenvalues and eigenfunctions. The evolution of any quantity can be expressed as a sum over these eigenfunctions. For example the energy time dependence is

$$E(t) = \sum_{mm'} c_m c^*_{m'} E_{mm'} \exp[i(\omega_m - \omega_{m'})t] \tag{112}$$

where $E_{mm'}$ are the matrix elements and the initial state is $\psi(n, 0) = \sum_m c_m \varphi_m(n)$. For chaotic motion the dependence is generally very complicated but the statistical properties of the evolution can be related to the statistics of eigenfunctions $\varphi_m(n)$ (and hence of the matrix elements $E_{mm'}$) and of eigenvalues ω_m.

There exists a well-developed random matrix theory (RMT) which describes some average properties of a typical quantum system with a given symmetry of the Hamiltonian. At the beginning the object of this theory was assumed to be a very complicated, particularly many dimensional, quantum system as a representative of a certain statistical ensemble. After understanding the phenomenon of dynamical chaos it became clear that the number of freedoms of the system is irrelevant. Instead, the number of quantum states or the quasi-classical parameter is of importance provided the dynamical chaos is in the classical limit.

Until recently ergodicity of eigenfunctions was assumed in this theory which means that in the expansion

$$\varphi_m = \sum_j^N a_{mj} u_j \tag{113}$$

where the u_j form a physically significant, for example unperturbed, basis all probabilities

$$< |a_{mj}|^2 >= \frac{1}{N} \tag{114}$$

are equal on average, and N is the size of the matrix. Under this condition the distribution of neighbouring level spacings is given approximately by the Wigner–Dyson law

$$p(s) \approx A s^\beta \exp(-B s^2) \tag{115}$$

where A, B are obtained from normalization and the condition $< s >= 1$. The repulsion parameter β takes three values only (1, 2, or 4) depending on system's symmetry.

A new problem here is the impact of localization on the level statistics. This was first addressed in Ref.[45], and a new class of semiempirical spacing distributions was discovered

$$p(s) \approx A s^\beta \exp\left[-\frac{\pi^2}{16}\beta s^2 - \left(B - \frac{\pi\beta}{4}\right) s\right] \tag{116}$$

where β is now a continuous parameter in the whole interval (0, 4). This distribution is also called the *intermediate statistics* in contrast to the *limiting statistics* (115) for the ergodic eigenfunctions. This intermediate statistics should be distinguished from that of Berry–Robnik [66] which describes the lack of ergodicity in the classical limit.

The repulsion parameter β was shown to be closely related to the entropy localization length [16], namely

$$\beta \approx \beta_{\overline{H}} = \beta_e \exp\left[\overline{H} - H_e(\beta_e)\right] = \frac{\gamma(\beta_e)}{N} l_{\overline{H}} \tag{117}$$

where $\beta_e = 1, 2, 4$ is the repulsion parameter for ergodic eigenstates with limiting statistics (115) and average entropy H_e. The reason for this simple relation remains an open question (see also below).

Unlike the statistical RMT, the intermediate statistics was introduced and studied in dynamical systems like the SM. The statistical counterpart of the latter is the band random matrix (BRM) theory recently developed [48] which was a revival of Wigner's old work [67]. In this theory an ensemble of matrices is considered whose non-zero elements occupy some band of width $2b$ around the main diagonal.

Indeed the one-period evolution of the kicked rotator, in the angular momentum representation, is given by a unitary $N \times N$ matrix. This matrix has a band structure of width $2k$. The ergodicity parameter which describes the statistical properties in the regime of full classical chaos is the ratio k^2/N. This similarity suggests that the appropriate ergodicity parameter in BRM theory is [46]

$$\lambda_r = r\frac{b^2}{N} \tag{118}$$

where r is some numerical factor. This was recently confirmed analytically in Ref.[53]. It turns out [46] that the scaling $\beta_{\bar{H}}(\lambda_r)$ is similar but not identical to that for the dynamical problem (47). In fact, in the region of small λ_r up to $\lambda_r \approx 3$, the dependence is the same with $r \approx 1.5$. The second region ($\beta_{\bar{H}} \approx 1$) is apparently different but it has not yet been studied in detail. Notice, that the origin of the difference can be attributed not so much to the distinction between "random" and "deterministic" matrix elements as to the different boundary conditions for a square matrix and a torus. The scaling in the first region was recently theoretically confirmed in Ref.[50]. However, no explanation for the observed deviations from this scaling at large λ_r was given.

A similar scaling behaviour was also found for tridiagonal symmetric matrices describing the Anderson and Lloyd models in disordered solids [49]. Unlike previous models, no deviations from the first scaling were observed, and the scaling was presented in a 'model-independent' form (cf. Eq.(48)):

$$\frac{1}{\xi_1(N, W)} = \frac{1}{\xi_1(\infty, W)} + \frac{1}{\xi_1(N, 0)} \tag{119}$$

where W is the disorder parameter. However, the scaling may depend on the imposed boundary conditions (in the latter two models zero boundary conditions were chosen).

Notice that for $\lambda_r << 1$ the matrix of eigenfunctions (113) is also a band matrix with a_{ij} smoothly decreasing off the diagonal, and with a much larger effective width $\sim b^2$.

Until recently homogeneous BRMs were studied which do not describe the global structure of conservative systems. Indeed, the level density ρ of such matrices grows indefinitely as $N \to \infty$. Clearly, N is an irrelevant (technical) parameter for a conservative system with its energy shells of a finite width ΔE. Instead, inhomogeneous BRM were introduced [52] with increasing diagonal elements (also considered by Wigner [67])

$$\langle H_{mn} \rangle = \frac{m \cdot \delta_{mn}}{\rho}; \qquad \langle H_{mn}^2 \rangle = \sigma^2, \; m \neq n \tag{120}$$

In such a model the localization length is bounded from above by the energy shell width [51–53]

$$l \leq l_\perp \approx 5.3 \, \sigma \rho \sqrt{b} \approx \rho \Delta E \tag{121}$$

After the introduction of the parameter

$$\lambda = \frac{l(0)}{l_\perp} \approx \frac{1.2 \, b^2}{l_\perp} \tag{122}$$

the scaling is described by the relation (cf. Eq.(47))

$$\beta_s(\lambda) = \frac{l(\lambda)}{l_\perp} = \lambda \, s(\lambda) \tag{123}$$

The scaling function $s(\lambda)$ was found numerically in Ref.[51] and has the following properties [52,53,64]: $s(0) = 1$, $\lambda \, s(\lambda) \to 1$ as $\lambda \to \infty$. In the latter case the localization length reaches the maximum, $l_\perp$, which corresponds to the ergodic eigenfunctions (within an energy shell). For this reason we call λ the ergodicity parameter, similar to the parameter (39) for an SM on a torus. Nevertheless, the eigenfunctions remain globally localized. We call this the *transverse localization* (across the energy shell) as contrasted to the *longitudinal localization* (along the shell) for $l < l_\perp$.

As was shown in Ref.[52] the parameter λ determines the level statistics. Moreover, using numerical data from this paper we have found [51] that the level repulsion parameter $\beta \approx \beta_s(\lambda)$ is again surprisingly close to the scaling function (Fig.11) (cf. Eq.(117)) in spite of the fact that the scaling itself is qualitatively different. Namely:

$$\beta_s(\lambda) \approx 1 - \exp(-\lambda) \tag{124}$$

in the whole range of available data ($0 < \lambda < 4$). Remarkably, this relation between statistical (β) and localization (β_s) characteristics of eigenfunctions has

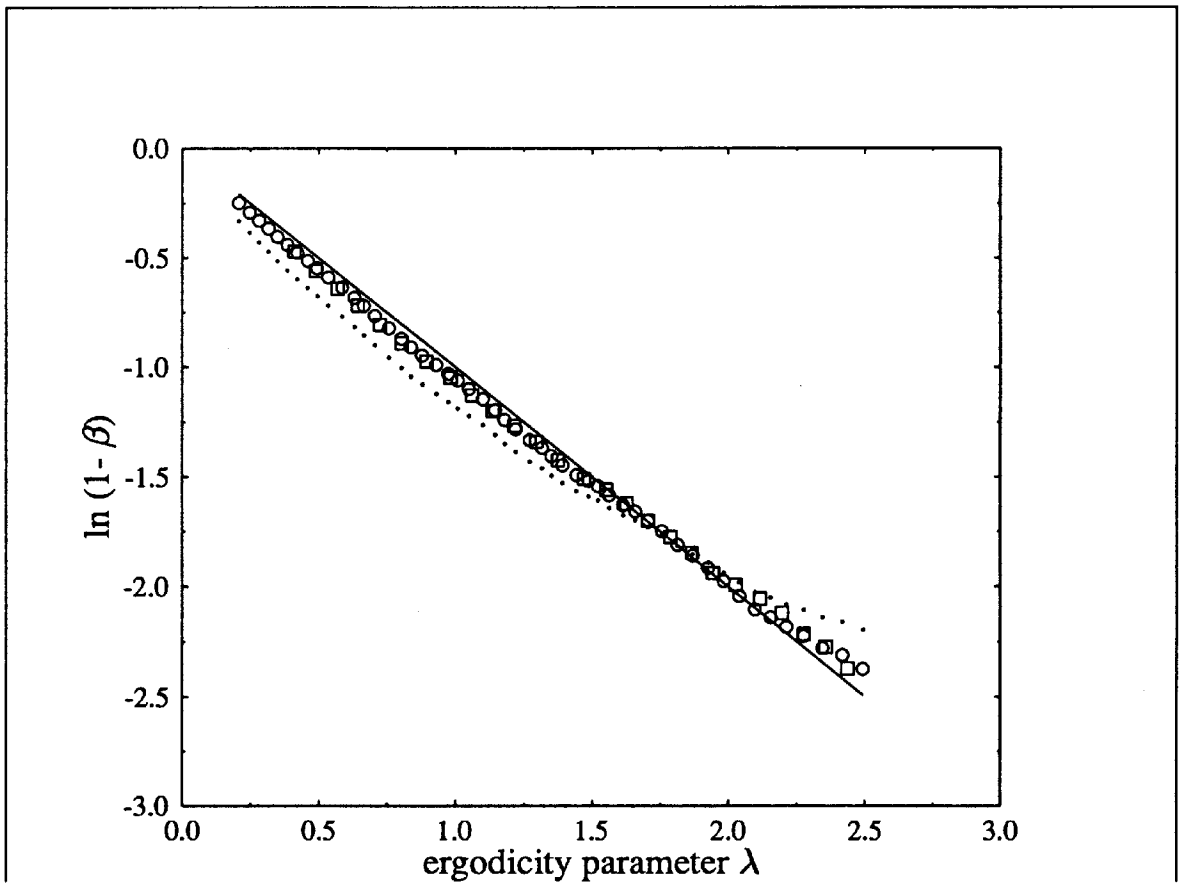

Fig. 11. The dependence of Brody's (points) and Izrailev's (circles) level repulsion parameters as well as of the localization parameter (squares) on the ergodicity parameter λ. The straight line is exponential scaling (124) (after Ref.[51]).

actually no fitting parameter. Yet, the scaling (124) may depend on the model via a particular structure of the energy shell, especially, of its borders.

Notice that the localization lengths ξ_q introduced in (44) depend on q and hence the surprisingly accurate relation $\beta \approx \beta_s$ holds for one localization length only namely the entropy localization length.

To conclude this section, we would like to attract the attention to a very interesting and less known theorem due to Shnirelman [37] (for the proof of both his theorems see Ref.[38]). It is related to KAM integrability in the classical limit which is intermediate between complete integrability with corresponding independent quantum levels (see Eq.(116), $\beta = 0$) and quantum chaos with level repulsion ($\beta \neq 0$). The classical KAM structure is highly intricate as its chaotic part, being of exponentially small measure, is everywhere dense. In quantum mechanics the beautiful Shnirelman theorem, which does not even need translation, asserts:

$$\forall N\, \exists C_N > 0, \quad \forall n > 1 \quad min(\lambda_{n+1} - \lambda_n, \lambda_n - \lambda_{n-1}) < C_N n^{-N} \tag{125}$$

where λ_n^2 are the energy eigenvalues. Thus, asymtotically as $n \to \infty$, a half of level spacings are exponentially small. A striking difference from both the complete integrability and quantum chaos!

10 Conclusion: some random remarks on quantum chaos

In a mathematical theory the definition of the main object of the theory procedes the results; in physics, expecially in new fields, it is quite often vice versa. First, one studies a new phenomenon, like dynamical chaos and only at a later stage, after understanding it sufficiently, do we try to classify it, to find its proper place in the existing theories and eventually to choose the most reasonable definition.

So far there is no common agreement, even among physicists, as to the definition of quantum chaos. The classical-like definition related to the exponential instability is not completely adequate since such a chaos is possible only in very exotic examples and does not describe typical quantum behaviour. On the other hand, the most popular definition, as some specific quantum properties for classically chaotic systems, seems to us also unacceptable (and even somewhat unhelpful) from the physical point of view. For example such a "chaos" may happen to be a perfectly regular motion in the case of perturbative localization discussed above.

In attempts to construct a more reasonable definition of quantum chaos, we would like to emphasize the most striking peculiarity of this phenomenon as discussed above, namely that all statistical properties of classical dynamical chaos are present in quantum dynamics but only within restricted and different time scales. Thus we think that the best definition of quantum chaos is: "*finite-time* dynamical chaos". In other words, this new phenomenon reveals an intrinsic complexity and richness of the motion with discrete spectrum which has long been considered as the most simple and regular. This is also true for any classical linear waves but the linearity of quantum equations is not an approximation as in classical physics but a fundamental and universal physical property.

The practical importance of statistical laws even for a finite time interval is in that they provide a relatively simple description of the *essential* behaviour for a very complicated dynamics. The existing ergodic theory of dynamical systems which is asymptotic in time seems to be inadequate to describe this new phenomenon properly. With the latter definition of quantum chaos we feel that a new ergodic theory is required which could analyse the finite time statistical properties of dynamical systems. Of course this is much more difficult than the asymptotic relations in the existing theory but we believe that otherwise it would be impossible adequately to describe the new and important phenomenon of quantum chaos.

Since quantum mechanics is commonly accepted as a universal theory, the phenomenon of classical dynamical chaos strictly speaking does not exist in nature. Nevertheless it is very important in the theory as the limiting pattern to compare with real quantum dynamics. It is instructive to compare the brand new phenomenon of quantum chaos with the old mechanism for statistical laws in the thermodynamic limit $N \to \infty$ which is the standard approach in traditional statistical physics both classical and quantum. Thus, for infinitely dimensional

quantum systems true chaos is possible and also non-physical. When we speak about the absence of true chaos in quantum mechanics, we mean finite, and even few-dimensional, systems.

It turns out that both mechanisms are very similar since for any finite N in the latter or q in the former, the dynamics is formally regular and in particular is characterized by a discrete spectrum. The main difference is in the nature of the large parameter N or q. The similarity comes from the fact that if any of these parameters is large, the motion is controlled by a large number of frequencies which makes it very complicated. The study of quantum chaos helps us to understand better the old mechanism for chaos in many-dimensional systems; particularly we conjecture the existence of characteristic time scales similar to those in quantum systems.

The direct relation between these two seemingly different mechanisms of chaos can be traced back in some specific dynamical models. One interesting example is the non-linear Schrödinger equation [47] (for another example see Ref.[69]). From a physical point of view this describes the motion of a quantum system interacting with many other freedoms whose state is expressed via the ψ function of the system itself (the so-called mean field approximation). This approximation becomes exact in the limit $N \to \infty$ which is a particular case of the thermodynamic limit. Therefore the mechanism for chaos in this system is the old one. On the other hand the non-linear Schrödinger equation has generally exponentially unstable solutions hence the mechanism of chaos here is the new one. Thus for this particular model both mechanisms describe the same physical process. We would like to emphasize that the true chaos present in these apparently few-dimensional models actually refers to an infinite-dimensional system.

Also, we would like to make a few comments on the problem of quantum measurement. Studies of quantum chaos suggest that it may have a close relation to this problem. First the measurement device is a macroscopic system for which the classical description is a very good approximation. In such a system true chaos with exponential instability is quite possible. The chaos in the classical measuring device is not only possible but unavoidable since the measuring system has to be, a highly unstable system; indeed, a microscopic intervention here produces a macroscopic effect. The importance of chaos for the quantum measurement is that it destroys the coherence of the initial pure quantum state to be measured converting it into an incoherent mixture. In the existing theories of quantum measurement this is described as the effect of external noise [93]. Chaos theory allows us to get rid of the unsatisfactory effect of the external noise and to develop a purely dynamical theory for the loss of quantum coherence (see also Ref.[68]). Unfortunately this is not yet the whole story. Indeed, besides the loss of coherence the most important effect of quantum measurement is the redistribution of probabilities $|\psi|^2$ according to the result of the measurement, the famous ψ-collapse, which remains to be explained. It seems that any dynamical explanation

of the ψ-collapse requires some changes in the existing quantum mechanics and this is the main difficulty both technical and philosophical.

In conclusion we would like to emphasize the importance of the so-called numerical experiments (the computer simulation of motion equations) in this as well as in many other fields of research. As a matter of fact, most information about non-trivial dynamics both classical and quantal has been gained in precisely this way, not in laboratory experiments. With all their obvious drawbacks and limitations numerical experiments have very important advantage as they provide complete information about the system under study. In quantum mechanics this advantage becomes crucial because in the laboratory one cannot observe (measure) the quantum system without causing a radical change of its dynamics. Nevertheless, we believe that laboratory experiments remain vitally important because the basis of numerical experiments – the fundamental equations of physics – may (and eventually will) be found to be incomplete or even incorrect. No matter how negligible the probability, in view of the thousands of experiments already done, any new possibility like quantum chaos should be used carefully to check the fundamental equations in the laboratory again and again.

REFERENCES

[1] A. Lichtenberg and M. Lieberman, *Regular and Stochastic Motion*, Springer, Berlin (1983); G.M. Zaslavsky, *Chaos in Dynamic Systems*, Harwood (1985).

[2] V.I. Arnold and A. Avez, *Ergodic Problems of Classical Mechanics*, Benjamin, New York (1968).

[3] I. Kornfeld, S. Fomin and Ya. Sinai, *Ergodic Theory*, Springer, Berlin (1982).

[4] V.M. Alekseev and M.V. Yakobson, Phys. Reports **75**, 287 (1981).

[5] B.V. Chirikov, in *Proc. 2d Intern. Seminar on Group Theory Methods in Physics*, Harwood (1985), Vol. 1, p. 553.

[6] J. Theiler, S. Eubank, A. Longtin, B. Galdrikian and J.D. Farmer, Physica D **58**, 77 (1992).

[7] B.V. Chirikov and V.V. Vecheslavov in *Analysis etc.*, Eds. P. Rabinowitz and E. Zehnder, Academic Press, New York (1990), p. 219.

[8] M. Berry, Proc.Roy.Soc.London A **413**, 183 (1987).

[9] J. Ford, G. Mantica and G. Ristow, Physica D **50**, 493 (1991).

[10] *Quantum Measurement and Chaos*, Eds. E. Pike and S. Sarkar, Plenum, New York (1987); *Quantum Chaos – Quantum Measurement*, Eds. P. Cvitanovic, I. Percival and A. Wirzba, Kluwer (1992).

[11] G. Casati, B.V. Chirikov, J. Ford and F.M. Izrailev, Lecture Notes in Physics **93**, 334 (1979), this volume.

[12] G. Casati et al, Phys. Reports **154**, 77 (1987); G. Casati, I. Guarneri and D.L. Shepelyansky, IEEE J. of Quantum Electr. **24**, 1420 (1988).

[13] F. Haake, *Quantum Signatures of Chaos*, Springer, Berlin (1991).

[14] F. Haake and D.L. Shepelyansky, Europhys.Lett. **5**, 671 (1988).

[15] Wei-Min Zhang and Da Hsuan Feng, Geometry on Quantum Non-Integrability (1992) (unpublished).

[16] F.M. Izrailev, Phys. Reports **196**, 299 (1990).
[17] G. Casati, J. Ford, I. Guarneri and F. Vivaldi, Phys. Rev. A **34**, 1413 (1986).
[18] D. Cohen, ibid. **44**, 2292 (1991).
[19] B.V. Chirikov, F.M. Izrailev and D.L. Shepelyansky, Sov. Sci. Rev. C **2**, 209 (1981); Physica D **33**, 77 (1988).
[20] G.P. Berman and G.M. Zaslavsky, Physica A **91**, 450 (1978).
[21] M. Toda and K. Ikeda, Phys. Lett. A **124**, 165 (1987); A. Bishop et al, Phys. Rev. B **39**, 12423 (1989).
[22] E. Wigner, Phys. Rev. **40**, 749 (1932); V.I. Tatarsky, Usp. Fiz. Nauk **139**, 587 (1983).
[23] D.L. Shepelyansky, Physica D **8**, 208 (1983); G. Casati et al, Phys. Rev. Lett. **56**, 2437 (1986); T. Dittrich and R. Graham, Ann.Phys. **200**, 363 (1990).
[24] K. Ikeda, this volume.
[25] A. Peres, in: *Quantum Chaos*, Eds. H. Cerdeira, R. Ramaswamy, M. Gutzwiller and G. Casati, World Scientific, Singapore (1991).
[26] B.V. Chirikov, D.L. Shepelyansky, Radiofizika **29**, 1041 (1986).
[27] G. Fusina, thesis, Physics Dept. Milan University (1992); G. Casati, B.V. Chirikov and G. Fusina, *Relaxation to the Quantum Steady State in the Kicked Rotator Model* (in preparation).
[28] N. Mott, Phil. Mag. **22**, 7 (1970).
[29] M. Berry, Proc. Roy. Soc. Lond. A **423**, 219 (1989).
[30] T. Dittrich and U. Smilansky, this volume.
[31] E. Heller, Phys. Rev. Lett. **53**, 1515 (1984).
[32] E.B. Bogomolny, Physica D **31**, 169 (1988).
[33] A.I. Shnirelman, Usp. Mat. Nauk **29**, #6, 181 (1974).
[34] R. Blümel and U. Smilansky, Phys. Rev. Lett. **69**, 217 (1992).
[35] F.M. Izrailev, private communication (1992).
[36] B.V. Chirikov, CHAOS **1**, 95 (1991).
[37] A.I. Shnirelman, Usp. Mat. Nauk **30** #4, 265 (1975).
[38] A.I. Shnirelman, On the *Asymptotic Properties of Eigenfunctions in the Regions of Chaotic Motion*, addendum in: V.F.Lasutkin, *The KAM Theory and Asymptotics of Spectrum of Elliptic Operators*, Springer, Berlin (1991).
[39] R. Jensen, Phys. Rev. Lett. **49**, 1365 (1982); Phys.Rev. A **30**, 386 (1984).
[40] R. Prange, D. Grempel and S. Fishman, this volume.
[41] D.L. Shepelyansky, Physica D **28**, 103 (1987).
[42] E.P. Nakhmedov et al, Zh. Eksp. Teor. Fiz. **92**, 2133 (1987).
[43] B.V. Chirikov, in: Proc. Les Houches Summer School on *Chaos and Quantum Physics*, Elsevier, North Holland, Amsterdam (1991).
[44] G. Casati and I. Guarneri, Comm. Math. Phys. **95**, 121 (1984).
[45] F.M. Izrailev, Phys. Lett. A **134**, 13 (1988); J. Phys. A **22**, 865 (1989).
[46] G.Casati et al, Phys. Rev. Lett. **64**, 1851 (1990); J. Phys. A **24**, 4755 (1991).
[47] F. Benvenuto et al, Phys. Rev. A **44**, R3423 (1991); G. Jona-Lasinio et al, Phys. Rev. Lett. **68**, 2269 (1992); D.L. Shepelyansky: Phys. Rev. Lett. **70**, 1787 (1993).
[48] T. Seligman et al, Phys.Rev.Lett. **53**, 215 (1985); M. Feingold et al, Phys. Rev. A **39**, 6507 (1989).
[49] G. Casati et al., J.Phys.: Condens. Matter **4**, 149 (1992).
[50] Ya.V. Fyodorov and A.D. Mirlin, Phys. Rev. Lett. **69**, 1093 (1992).

[51] G. Casati, B.V. Chirikov, I. Guarneri and F.M. Izrailev, Phys. Rev. E. **48**, R1613 (1993).
[52] M. Wilkinson, M. Feingold and D. Leitner, J. Phys. A **24**, 175 (1991); Phys. Rev. Lett. **66**, 986 (1991).
[53] Ya.V. Fyodorov and A.D. Mirlin, Phys. Rev. Lett. **67**, 2405 (1991).
[54] M. Berry, J. Phys. A **10**, 2083 (1977); A. Voros, Lecture Notes in Physics **93**, Springer, Berlin (1979), p. 326.
[55] P. O'Connor and E. Heller, Phys. Rev. Lett. **61**, 2288 (1988); P. Leboeuf et al, Ann. Phys. **208**, 333 (1991).
[56] S. Weigert, Z. Phys. B **80**, 3 (1990); M. Berry, *True Quantum Chaos? An Instructive Example*, Proc. Yukawa Symposium, 1990; F. Benatti et al, Lett. Math. Phys. **21**, 157 (1991); H. Narnhofer, J. Math. Phys. **33**, 1502 (1992).
[57] M. Born, Z. Phys. **153**, 372 (1958); G. Casati, B.V. Chirikov and J. Ford, Phys. Lett. A **77**, 91 (1980).
[58] D.V. Anosov, Dokl. Akad. Nauk SSSR **145**, 707 (1962).
[59] G. Casati, B.V. Chirikov, G. Fusina and F.M. Izrailev, *The Structure of Mott's States* (in preparation).
[60] B.V. Chirikov and F.M. Izrailev, *Statistics of Chaotic Quantum States: Localization and Entropy* (in preparation).
[61] E.V. Shuryak, Zh. Eksp. Teor. Fiz. **71**, 2039 (1976).
[62] F.M. Izrailev and D.L. Shepelyansky, Teor. Mat. Fiz. **43**, 417 (1980).
[63] A. Rechester et al, Phys. Rev. A **23**, 2664 (1981).
[64] A. Gioletta, M. Feingold, F.M. Izrailev and L. Molinari, Phys. Rev. Lett. **70**, 2936 (1993).
[65] N. Ben-Tal et al, Phys. Rev. A **46**, #3 (1992).
[66] M. Berry and M. Robnik, J. Phys. A **17**, 2413 (1984).
[67] E. Wigner, Ann.Math. **62**, 548 (1955); **65**, 203 (1957).
[68] L. Bonci et al, Phys. Rev. Lett. **67**, 2593 (1991).
[69] G.P. Berman and G.M. Zaslavsky, this volume.
[70] F. Delyon, B. Simon and B. Souillard, Ann.Inst.; H.Poincaré **42**, 283 (1985).
[71] F. Benvenuto, G. Casati, I. Guarneri and D.L. Shepelyansky, Z. Phys. B. **84**, 159 (1991).
[72] P.W. Anderson, Phys. Rev. **109**, 1492 (1958).
[73] D. Dunlap et al., Phys. Rev. Lett. **65**, 88 (1990).
[74] D.J. Thouless, J. Phys. C: Solid State Phys **5**, 77 (1972).
[75] H. Schmidt, Phys. Rev. **105**, 425 (1957).
[76] G. Casati and L. Molinari, Prog. Th. Physics suppl. **98**, 287 (1989).
[77] G. Casati, I. Guarneri and D.L. Shepelyansky, Physica A **163**, 205 (1990).
[78] P.A. Lee and T.V. Ramakhrishnan, Rev. Mod. Phys. **57**, 287 (1985).
[79] D.L. Shepelyansky, Physica **D 8**, 208 (1983).
[80] E. Abrahams, P.W. Anderson. D.C. Licciardello and T.V. Ramakrishnan, Phys. Rev. Lett. **42**, 673 (1979).
[81] G. Casati, I. Guarneri and D.L. Shepelyansky, Phys. Rev. Lett. **62**, 345 (1989).
[82] J.E. Bayfield and P.M. Koch, Phys. Rev. Lett. **33**, 258 (1974).
[83] J.C. Leopold and I.C. Percival, Phys. Rev. Lett. **41**, 944 (1978).
[84] F. Benvenuto, G. Casati and D.L. Shepelyansky, Phys. Rev. A **47**, R786 (1993).

[85] N.B. Delone, B.P. Krainov and D.L. Shepelyansky, Sov. Phys. Usp. **26**, 551 (1983).
[86] G. Casati, B.V. Chirikov and D.L. Shepelyansky, Phys. Rev. Lett. **53**, 2525 (1984).
[87] G. Casati and I. Guarneri, Comments Atomic Molecular Physics, **25**, 185 (1991).
[88] G. Casati, I. Guarneri and D.L. Shepelyansky, Chaos, Solitons and Fractals **1**, 131 (1991).
[89] E.J. Galvez, B.E. Sauer, L. Moorman, P.M. Koch and D. Richards, Phys. Rev. Lett. **61**, 2011 (1988).
[90] J.E. Bayfield, G. Casati, I. Guarneri and D.W. Sokol, Phys. Rev. Lett. **63**, 364 (1989) (this volume).
[91] R. Artuso, G. Casati and D.L. Shepelyansky, Phys. Rev. Lett. **68**, 3826 (1992).
[92] R. Artuso, F. Borgonovi, I. Guarneri, L. Rebuzzini, G. Casati, Phys. Rev. Lett. **69**, 3302 (1992).
[93] J.A. Wheeler, W.H. Zurek Eds., Quantum Theory and Measurement, Princeton Univ. Press, Princeton (1983).
[94] P. Leboeuf, J. Kurchan, M. Feingold and D.P. Arovas, Phys. Rev. Lett. **65**, 3076 (1990); R. Lima and D.L. Shepelyansky, Phys. Rev. Lett. **67**, 1377 (1991); T. Geisel, R. Ketzmerick and G. Petschel, Phys. Rev. Lett. **66**, 1651 (1991); **67**, 3635 (1991).